New observations of the Spreading and Variability of the Antarctic Intermediate Water in the Atlantic

Claudia Schmid and Silvia L. Garzoli

National Oceanic and Atmospheric Administration, Atlantic Oceanographic and Meteorological Laboratory, Miami, Florida, USA

in press
to appear in November issue of
Journal of Marine Research

- 29 January 2010 -

Corresponding author address: Dr. Claudia Schmid, NOAA/AOML/PHOD, 4301 Rickenbacker Causeway, Miami, FL 33149, USA

Abstract

The new and unique Argo data set currently available, in conjunction with other data previously collected, allowed to increase our understanding of the spreading of the Antarctic Intermediate Water in the southern and tropical Atlantic Ocean and to verify previous results. The combination of velocity and salinity data collected with Argo floats verified the main patterns of circulation at intermediate (800 to 1100 dbar) depths. Interesting new features in the pathways are found: (1) the existence of a new, third, branch of westward to northwestward flow that is fed by the Benguela Current; (2) two pathways through which the water from the Benguela Current Extension feeds into the Intermediate Western Boundary Current, one turns north at the western boundary while the other one turns north about 10° farther offshore; (3) the core of the South Atlantic Current is located farther north than was thought earlier (at 35 to 38°S instead of south at about 40°S); (4) significant flow of water from the South Atlantic Current to the Antarctic Circumpolar Current occurs east of the Zapiola Eddy (at about 45°S, 35°W); (5) a quite robust eastward current exists at about 20°S; and (6) there are indications, only in the salinity distribution, for southward spreading of Antarctic Intermediate Water from the equator near the eastern boundary.

Transport estimates for the 800 to 1100 dbar layer show that the transports of the zonal currents in the subtropical gyre at intermediate depth increase from east to west, and that this trend is nearly linear. The transport of the South Atlantic Current near the western boundary is between 5 and 10 Sv, while it is close to 1 Sv near the eastern boundary of the Atlantic. The transport of the Benguela Current Extension is about 8 Sv near 45°W and only about 1 Sv near 14°E. It is also found that at the bifurcation of the Benguela Current Extension (at 28.5°S) about two thirds of the Antarctic Intermediate Water recirculate in the subtropical gyre, which is a smaller portion than the three quarters reported previously. Zonally integrated transports in the Antarctic Intermediate Water layer show that, as a meridional average, about 3 Sv are transported northward in the 800 to 1100 dbar layer. At 35°S this transport is 2.8 Sv, which amounts to 16% of the total northward transport of the Meridional Overturning Circulation (18 Sv).

An analysis of the variability shows that the confluence of the Malvinas Current and the Brazil Current undergo seasonal variations at intermediate depth. The confluence is at its northernmost location (36°S) in July-September. On average the confluence is at 38°S. Both, the variability and the mean location of the confluence at the depth of Antarctic Intermediate Water is similar to what has been observed at the surface.

1 Introduction

The Antarctic Intermediate Water (AAIW) is characterized by a salinity minimum below the thermocline that is found north of the Subantarctic Front (for descriptions of fronts in the southern ocean see, e.g., Belkin and Gordon, 1996; Orsi et al., 1995). This water mass, plays an important role in the South Atlantic and in the global ocean circulation since it contributes significantly to the northward flow of the upper limb of the Meridional Overturning Circulation (e.g. Rintoul, 1991).

Early studies which looked at the characteristics and spreading of the AAIW in the Atlantic Ocean were based on hydrographic data sets of quite coarse resolution, and based their results on the circulation primarily on the changes of the water properties at the depth of the subsurface salinity minimum (Deacon, 1933; Wüst, 1935; Defant, 1941). The main conclusion of these studies was that the AAIW originates in the southern South Atlantic and primarily spreads to the north along the western boundary.

More recent studies used hydrographic observations to derive the circulation using the geostrophic balance (Reid, 1989; Suga and Talley, 1995) or Lagrangian observations that covered mostly the western basin, the Agulhas/Benguela Region and the tropical Atlantic (Boebel et al., 1999; Boebel et al., 2003; Richardson and Garzoli, 2003). These studies showed that the AAIW originates from the southern Subantarctic Front. There are two source water masses that feed into the AAIW found in the Atlantic Ocean. One of them is the Subantarctic Mode Water, which is formed in the Pacific Ocean and enters the southwest Atlantic through the Drake Passage. This water mass is found south of the Subantarctic Front. The second one is AAIW of Indian Ocean origin that flows into the eastern South Atlantic via the Agulhas/Benguela Current system.

A portion of the Subantarctic Mode Water from the Pacific Ocean flows northward in the Malvinas Current and subducts to become AAIW, while most of the Subantarctic Mode Water continues eastward in the Antarctic Circumpolar Current. Another area of subduction of Subantarctic Mode Water into the AAIW layer is the region just south of the Subantarctic Front (the Polar Front Zone) throughout the whole Atlantic Basin (Schmid et al., 2000). The northward Malvinas Current meets the southward Brazil Current at approximately 38°S (Garzoli and Bianchi, 1987; Olson et al., 1988) in what is called the Confluence (Gordon and Greengrove, 1986). This region is characterized by a strong thermohaline front at the surface, because the Malvinas Current transports fresh and cool water, whereas the Brazil Current transports warmer and saltier water.

From the Confluence the AAIW flows eastward in the South Atlantic Current/Antarctic Circumpolar Current system. According to You et al. (2003) 86% of the AAIW originating from the Drake Passage

continues into the Indian Ocean while the rest of it mixes with water of Indian Ocean origin in the Cape Basin and feeds into the Benguela Current. Most of this water then continues westward around 30°S in the Benguela Current Extension which bifurcates at the western boundary. This bifurcation has been called the Santos Bifurcation by Boebel et al. (1999). Schmid et al. (2000) found that three quarters of the water reaching the bifurcation at intermediate depth recirculates southward to the Confluence. It has been shown that this anticyclonic basin-wide flow pattern is part of the subtropical gyre of the South Atlantic (Schmid et al., 2000). The northward branch originating at the bifurcation continues all the way to the equator and beyond (e.g. Boebel et al., 1999). This current is called the Intermediate Western Boundary Current up to about 6°S. Farther north this boundary current becomes part of the North Brazil Current.

The mean and the variability of the flow at intermediate depth in the subtropics, including in the confluence regions are not well know. The variability in the confluence region is likely to be significant, since several studies of the surface Confluence established that a seasonal variability exists that is related to the curl of the wind stress in the region. These studies used sea surface temperature (Olson et al., 1988), satellite altimetry (Goni and Wainer, 2001) and observations from instruments at the ocean bottom (Garzoli and Bianchi, 1987; Garzoli and Garraffo, 1989). It seems likely that a similar variability exists at the depth of the AAIW because CTD data in the area (e.g. Gordon and Greengrove, 1986), around 38°S west of 54°W, show a thermohaline stratification characteristic of the Malvinas Current, the southward retroflection of the Malvinas Current, and a Brazil Current that reaches down to about 1400 m.

North of the subtropical region, especially in the equatorial region, the flow pattern at intermediate depths consists of many narrow zonal currents (e.g. Stramma and Schott, 1999; Schmid et al., 2003, Ollitrault et al., 2006). At 6°S enough data were available to determine that the flow is dominated by variability consistent with planetary waves, one of which causes reversals of the flow (Schmid et al., 2003).

In this study we use quasi-Lagrangian and hydrographic observations, mostly from profiling floats, and Lagrangian observations from floats that can be tracked under water to get a more complete picture of the spreading and transports of the water at intermediate depth. Signs of seasonal variability of the flow will be investigated in a subtropical region where the data coverage is sufficient.

2 Data and Methods

Data from profiling floats and CTDs collected during January 2006 through December 2008 are used to derive the hydrographic properties of the AAIW. The primary sources for the float profiles are the

Argo Global Data Centers[3]. Some additional float profiles as well as the data from other instruments are available through the Global Telecommunication System (GTS) used by the meteorological and oceanographic community. For this work the profiles were retrieved from the Global Temperature and Salinity Profile Program (GTSPP) at NODC (National Oceanographic Data Center).

Profiles from Argo floats pass through various quality control procedures. The real-time tests are automatic and standardized[4]. Profiles collected by the US Argo Data Assembly Center (Schmid et al., 2007) are also compared with the NCEP ocean reanalysis (Global Ocean Data Assimilation System, GODAS, Dave Behringer, NCEP, personal communication, 2005) and the most recent version of the World Ocean Atlas. Currently the World Ocean Atlas of 2005 is used (Antonov et al., 2006; Locarnini et al., 2006). Based on the outcome of these two comparisons the profiles are inspected visually, which helps in the detection of sensor drifts or offsets. A similar quality control procedure is applied to all CTD profiles that were acquired from GTSPP.

To obtain gridded fields, the data are grouped into 5° longitude by 1.5° latitude boxes. Then the pressure and temperature at the depth of the salinity minimum are derived for each profile. An additional quality control is performed on the properties of the AAIW through a statistical analysis of the salinity, temperature and pressure. If a value is outside of 2 standard deviations around the median of all values in each box for the month of observation it is considered unreliable and excluded from the analysis. In cases with too few observations within one box, this quality control uses observations from immediately adjacent boxes as well. After these procedures are completed most of the study region is covered with observations and the majority of the boxes have 20 observations or more (Fig. 1, top). The data that passed the quality control are used to derive monthly mean fields for each year which are, in turn, used to derive monthly climatological fields. The next step is an objective analysis that produces fields of the hydrographic properties with a grid resolution of 1° by 1° (Hiller and Käse, 1983). These fields in turn are used to estimate the annual mean of the hydrographic properties.

Trajectories from quasi-Lagrangian and Lagrangian floats covering the 1989 to 2009 period are used to derive the velocity field at intermediate depth, between 800 and 1100 dbar. This pressure range was chosen, because the majority of floats drift within that range, and because this pressure range overlaps with the pressure range where the Antarctic Intermediate Water is found in large parts of the Atlantic. Trajectory data outside this pressure range are excluded from the analysis. The float data collected during the World Ocean Circulation Experiment (WOCE) cover the time period from

[3]US Global Ocean Data Assimilation Experiment and Coriolis in France, with the web pages www.usgodae.org/argo/argo.html and www.coriolis.eu.org//cdc/argo.htm

[4]A document describing the Argo quality control tests is available at www.coriolis.eu.org//cdc/argo_rfc.htm; the main tests are: speed check, gross range tests, spike tests, pressure increasing test, and a vertical gradient test.

January 1989 to December 2000 and include Autonomous Lagrangian Current Explorer (ALACE) and RAFOS floats (RAFOS = Ranging And Fixing Of Sound). The data from profiling floats cover the time period from July 1997 to June 2009. These data are used to derive velocity estimates from each float that are normalized to reflect daily observations[5]. This step is necessary to allow the derivation of average velocities from floats that sample the ocean with different temporal resolutions without introducing a bias towards measurements from floats that have a higher sampling frequency.

The largest numbers of daily velocity estimates are available north of about 40°S between 45 and 10°W and in the area around 30°S, 10°E (Fig. 1, middle). Other areas with relatively large data densities are the region south of the Brazil-Malvinas Confluence (around 38°S, 50°W) and the Agulhas region including the Agulhas Retroflection (south of 35°S between 5 and 30°E). In these two regions the number of floats is largest (Fig. 1, bottom). Other areas with relatively large numbers of floats are around 30°S, 10°E, in the region of the Drake Passage (near the western boundary, 55 to 60°S), in the Malvinas Current and its extension (near the western boundary, 40 to 50°S), and in the western tropical Atlantic (within about 10° of the equator, especially along the western boundary in the North Brazil Current).

The velocities in the 800-1100 dbar layer derived from these Lagrangian and quasi-Lagrangian observations are used to derive quarterly (January-March, ...) means of the velocity and the transport on a 1° by 1° grid. In the next step, an objective analysis is performed, similar to the one used for the hydrographic fields and with the same grid resolution (1° by 1°). The annual mean is then derived from the quarterly fields to reduce the seasonal bias that can be introduced by a data coverage that varies significantly from month to month. This approach is used for the box averaged and the objectively analyzed fields. The transports derived from the former are used in the boundary current regimes, while those derived from the latter are used in the interior.

Uncertainties of the transports, due to the fact that floats are drifting at various depths between 800 and 1100 dbar, are determined by calculating the geostrophic shear in this layer from the hydrographic observations. This uncertainty will be called the shear-based error in the following. As an additional measure of the uncertainty the standard deviation of the transports is derived. Another source of uncertainty exists for the profiling floats. It is introduced by the fact that a few hours can elapse between the time they reach (leave) the surface and the time it takes to get the first (last) position of the surface drift. The error associated with the time spent on the surface is quite small. Quantitative comparisons of the surface and subsurface displacements show that: (1) this error is less than 5% in the majority of cases, and (2) this error is less than 10% in about 80% of the cases. In contrast to

[5]Examples: (a) if a float provides three velocities per day we derive daily averages; (b) if a float provides a velocity every N days we end up with N velocities that are all the same. N is typically 10 or 7 days.

this, the statistical and shear-based errors are typically larger than 10% (in 75% and 55% of the cases, respectively).

The output of a simulation produced with the Hybrid Coordinate Ocean Model (HYCOM; Bleck, 2009; Chassignet et al., 2003; Halliwell, 2004) is used for model-data comparisons with the goal to use the model fields to understand the observed variability better. HYCOM is a generalized (hybrid) vertical coordinate primitive equation ocean model, which describes the ocean as a stack of fluid layers that are isopycnal in stratified regions, terrain following in shallow coastal regions and isobaric in the unstratified mixed layer. Thus, HYCOM preserves the advantages of isopycnal models in eliminating unrealistic diapycnal mixing due to truncation errors, while allowing the low-density layers in near-surface waters to become pressure-like in order to resolve the surface mixed layer.

The model covers the global domain at 1/12° resolution (with approximately 9 km resolution near the equator and 6 km in mid-latitudes), with a grid on a Mercator projection from 79°S to 47°N, and a bipolar patch north of 47°N. The model has 32 vertical layers based on potential density referenced at 2000 dbar (σ_2) with thermobaricity. The simulation was initialized from climatology (GDEM3, Teague et al., 1990; Carnes, 2003) and was spun up with ERA40 (Uppala et al., 2005) winds plus 6-hourly anomalies. The thermal fields were extrapolated from ocean values. The wind stress fields were corrected through a correlation with satellite winds (Metzger, personal communication). The model was spun up for 15 years, and the mean output from years 11 to 15 is used.

3 Mean water properties of Antarctic Intermediate Water

As was mentioned in the introduction, the AAIW is characterized by a salinity minimum below the thermocline that is found north of the Subantarctic Front. South of the Subantarctic Front another water mass, the Subantarctic Mode Water, is found. This water mass is characterized by a salinity minimum that is at or very close to the surface. The AAIW is formed when Subantarctic Mode Water subducts at the Subantarctic Front and in the northward Malvinas Current. Figure 2 shows the rapid deepening of the salinity minimum associated with this subduction near 40°S in the west and near 43°S in the east.

Areas where the pressure at the salinity minimum exceeds 870 dbar are observed in the Agulhas region (north of 40°S, east of 15°E) and near the center of the subtropical gyre (between 35 and 26°S west of the Greenwich Meridian, Fig. 2). The western region of high pressures is widening from east to west and has a maximum of 943 dbar at 32°S, 36°W. This pattern is consistent with the subtropical gyre dynamics that give rise to anticyclonic flow down to intermediate depths (Schmid et al., 2000). A region of high pressures is visible near the eastern boundary of the domain, south of Africa. The

largest value of 1027 dbar is found at 29°E, where the AAIW of Indian Ocean origin approaches the Atlantic. Most of this water returns to the Indian Ocean after going through the Agulhas Retroflection.

North of 30°S (Fig. 2) two basin-wide minima of the pressure (with less than 700 dbar, one is around the equator and the other extends from about 15°S in the west to about 25°S in the east) and two basin-wide maxima of the pressure (with about 800 dbar, one is around the 8°S and the other is near 10°N) exist. Similar results were obtained by You (2002) who observed that the isoneutral surface 27.40, which is representative for the depth of the salinity minimum, is relatively shallow around 15°S and relatively deep around 10°S. The zonal to quasi-zonal orientation of the isolines between the maxima and minima indicate that zonal currents play a major roll in the spreading of the AAIW in the interior, which is consistent with results from earlier studies (e.g. Talley, 1996; Stramma and Schott, 1999; Boebel et al., 1999; Schmid et al., 2003; Núñez-Riboni et al., 2005).

The salinity at the salinity minimum indicates the primary pathways of the spreading of the AAIW (Fig. 3). Along the western boundary, fresher water (salinity less than 34.1 psu) is spreading northward in the Malvinas Current and meets saltier water, which is spreading southward in the Brazil Current, in the confluence region at approximately 38°S.

As described in the introduction part of the Subantarctic Mode Water flows northward in the Malvinas Current and subducts to form the AAIW. Many floats follow the pathway of the Malvinas Current and its retroflection at the Confluence with the Brazil Current. The hydrographic data collected by these floats show the changes of the water mass distributions along the way. An example of this is depicted by float 3900426 (Fig. 4). The float was deployed in the South Pacific west of the Drake passage, followed the Antarctic Circumpolar Current and the Malvinas Current before it continued east after the confluence of the Malvinas Current and the Brazil Current (Fig. 4b). The first five profiles (2 black, 2 dark blue, 1 lighter blue, Fig. 4c) indicate that the float transitions between water masses (because it is a quasi-Lagrangian float). The profiles collected along the 1000 m isobath (Fig. 4a), have the freshest water with a salinity of less than 34.1 psu at the surface (Fig. 4c and e). After the confluence with the Brazil Current the near-surface salinity increases strongly, by about 1.8 psu, while the salinity near 300 dbar (the depth where the salinity minimum is located in the Confluence region) increases only temporarily by about 0.2 psu to 34.3 psu. For this one profile the float is in the regime dominated by subtropical water. As the float turns back to the south (Fig. 4a) the near-surface and subsurface salinity decrease slowly by about 1 psu and 0.1 psu (Fig. 4c), respectively.

From 25°S to 10°S and from the equator to 10°N a strong tongue of relatively fresh AAIW can be seen along the western boundary, indicating northward spreading of this water mass. In between these two regions, from about 10°S to the equator, no tongue of low salinity is visible along the western bound-

ary. Instead, there is a strong eastward tongue of relatively low salinity at 6°S and another weaker one at about 2°S. Between them, at 4°S, is a less pronounced tongue of higher salinity extending to the west. Earlier studies indicate that a narrow band of northward flow exists along the western boundary between 10°S and the equator (e.g. Talley, 1996; Stramma and Schott, 1999). Talley (1996) reported a tongue of low salinity (less then 34.4 psu) extending from 10°S to beyond 5°S (their Fig. 3). Such a tongue is not present in the salinity field based on the recent data (Fig. 3). It seems likely that this difference is due to insufficient coverage of the region with near-shore data collected in the time period studied here. In addition to this, the erosion of the salinity signal carried by such a current, through horizontal mixing with water carried westward at 4°S and through vertical mixing, is likely to be significant. This makes it impossible to resolve this weak and variable western boundary current between 10°S and the equator in the data set containing only recent hydrographic observations (see section 2).

At the eastern boundary the salty AAIW of Indian Ocean origin enters the Atlantic at 35°S, 15°E. From there it spreads northward to almost 30°S while losing much of its signature. Another interesting feature near the eastern boundary is the area of relatively high salinity centered at 8°S, 5°E which indicates that little horizontal exchange of water occurs. This lack of ventilation in the shadow zone of the ventilated thermocline (Luyten et al., 1983) allows an erosion of the salinity minimum by vertical mixing (e.g. Gordon and Bosley, 1991). In this region the Angola Gyre has been described as a feature that dominates the flow at the surface and in the thermocline (e.g. Stramma and Schott, 1999). It seems likely, from these observations, that the Angola Gyre has a significant impact on the flow in the AAIW layer.

4 Mean circulation at 800 to 1100 dbar

In order to determine to what extent the layer under study, 800 to 1100 dbar, is representative of the AAIW, an analysis was performed for two meridional transects by deriving the annual mean of the pressure at the salinity minimum as well as the potential densities and neutral density boundaries characterizing the AAIW layer (Fig. 5). Results from this analysis indicate that the layer includes the core of the AAIW layer in the subtropical gyre of the South Atlantic and in the Agulhas region south of South Africa (Fig. 2 and 5). Farther south, approximately south of 44°S, the AAIW layer is shallower than the layer where the floats are drifting (this area is indicated by hatching in Fig. 5). In the subtropical gyre the AAIW layer is best defined by the potential density surfaces 27.00 and 27.35 $kg\,m^{-3}$ (Fig. 5, top) and extends beyond the pressure levels used to derive the velocity field. Farther north, the core of the AAIW layer is slightly above 800 dbar (Fig. 2). Here the AAIW layer is best defined by the neutral density surfaces 27.25 and 27.55 $kg\,m^{-3}$ (Fig. 5, bottom). Figure 5 shows that the 800 to 1100 dbar layer in this region includes a significant portion of the AAIW layer (shaded

in grey). In addition, the geostrophic shear at this depth horizon is mostly quite small (see below), and therefore the velocities derived from floats drifting at some depth within the 800 to 1100 dbar layer can be considered as representative of the spreading of the AAIW in the subtropical and tropical Atlantic Ocean. The velocity field is used to derive the annual mean of the zonal and meridional transports and their errors in the 800 to 1100 dbar layer, as described in section 2. In the following the spreading of the water in this layer will be analyzed.

The annual mean velocities between 800 and 1100 dbar derived from quarterly mean fields of the velocity are shown in Figure 6. The zonal and meridional transports in this layer are shown in Figure 7 as a function of latitude (Fig. 7, top) and longitude (Fig. 7, bottom). Mean transports, as well as standard deviations and shear-based errors for various currents are given in Figures 8 and 9.

a. Subtropical Gyre

The water that is entering the Atlantic Ocean through the Drake Passage and feeding the nearly barotropic Malvinas Current can be clearly seen in Figure 6. In the mean the Malvinas Current, which can be found near the western boundary at 45°S in Figure 7 (bottom panel), carries a northward subsurface transport of 10.5 Sv (Fig. 9c) with a standard deviation of 1.9 Sv and a shear-based error of 3.4 Sv (1 Sv is $10^6 m^3 s^{-1}$). The mean subsurface southward transport associated with the Brazil Current, which can be found near the western boundary at 30 and 35°S in Figure 7 (bottom panel), is 5.2 Sv (Fig. 9c) with a standard deviation of 2.2 Sv and a shear-based error of 1.8 Sv. The Confluence of these two currents occurs at 38°S at 800 to 1100 dbar (Fig. 6), which supports the interpretation of the salinity field (see section 3 and Fig. 3). At the surface, the mean location of the retroflection of the Malvinas Current was found at the same latitude (e.g. Olson et al., 1988; Garzoli and Garraffo, 1989)

After the Confluence the water spreads eastward in a large meander that has its southernmost point at about 45°S, 55°W. Most of the eastward transport is carried by the Antarctic Circumpolar Current with a portion of the flow joining the South Atlantic Current. A striking feature in this region is the Zapiola Eddy (Flood and Shor, 1988; Davis et al., 1996), which is clearly represented in the velocity field (50 to 40°S, 55 to 30°W, Fig. 6, bottom). This strong anticyclonic eddy is located between the South Atlantic Current and Antarctic Circumpolar Current. East of the Zapiola Eddy, between 35 and 25°W, the South Atlantic Current splits up. A large part of the water flows in an east-southeasterly direction and continues eastward south of 40°S and joins the Antarctic Circumpolar Current, while a smaller part of the water continues toward South Africa as the South Atlantic Current. The broad strong Antarctic Circumpolar Current leaves the South Atlantic south of 42°S, whereas the considerably weaker South Atlantic Current continues to about 14°E and then feeds into the westward return

current of the subtropical gyre. This current is called the Benguela Current Extension (Richardson and Garzoli, 2003).

The eastward transport of the South Atlantic Current and the westward transport of the Benguela Current Extension are shown as a function of longitude in Figure 10. The lower panel shows the main core and the meridional boundaries of these currents, which can also be detected in Figure 7 (top panel). The southern boundary South Atlantic Current was determined by following the eastward flow north of the Zapiola Eddy, the separation from the Antarctic Circumpolar Current was based on the presence of boxes with a minimum in the eastward velocity or westward velocity. The northern boundary of the Benguela Current Extension was determined in a similar way (i.e. the velocity was eastward or only weakly westward). Their transports vary from longitude to longitude by up to 5 Sv, which is likely to be due to a combined effect of mesoscale variability and uneven sampling, and there is a strong indication that they have a significant longitude-dependent trend. Both transports decrease from west to east. The transport of the South Atlantic Current west of 30°W ranges from 3 to 10 Sv with the maximum at 40°W. Between 30 and 18°W the transport is between 3 and 5 Sv. East of 18°W the transport does not exceed 3 Sv and is about 1 Sv at the eastern boundary of the Atlantic. The standard deviation ranges from 0.5 Sv in the interior to 6.4 Sv near the boundary and the shear-based error ranges from 0.1 to 1.5 Sv (Fig. 8). The large range of the transport west of 30°W could be due to a high variability in the location of the meander originating in the Brazil-Malvinas Confluence. The west-to-east decrease of the transport is highlighted by the linear fit with a slope of -0.09 Sv per degree, which is shown as a dashed line in Figure 10. Based on this fit, the transport of the South Atlantic Current decreases from 5.7 Sv at 50°W to 0.2 Sv at 14°E.

The westward transport of the Benguela Current Extension increases from 1 Sv in the east to 8 Sv in the west (Fig. 10). Based on the linear fit the increase is from 2.5 to 6.7 Sv. The linear trend is smaller than for the South Atlantic Current, with a slope of 0.07 Sv per degree. However, within the margin of errors in the transport estimates, the transports of these currents are essentially the same. Both for the South Atlantic Current and the Benguela Current Extension the rings shed in the Agulhas Retroflection are likely to be responsible for the larger standard deviations observed east of about 5°E (Fig. 8a and b).

The longitude dependence of the transport for both currents could be explained by northward flows in the interior of the subtropical gyre which are generated by small recirculation cells (Fig. 6, top), e.g., between 10°W to 6°E (2.9 Sv on average for 36 to 33°S, Fig. 9a).

b. Flow along the eastern boundary

The northward flow associated with the Benguela Current at the surface is observed east of the Walvis Ridge (3°E, marked by WR in Fig. 2) at 30°S (Garzoli and Gordon, 1996). At the AAIW level this current is narrower than at the surface. It is observed between 8 and 12°E at 34°S and between 9 and 13°E at 33°S. At 34 and 33°S, the observations reveal a southward flow east of the Benguela Current (Fig. 9b), which confirms earlier reports of such a countercurrent (e.g. Richardson and Garzoli, 2003). The water in this current retroflects to join the Benguela Current, which turns to the west to feed into the Benguela Current Extension. The latter current flows westward along approximately 30°S (Fig. 10) and bifurcates at the western boundary, near 28.5°S (in the Santos Bifurcation, Boebel et al., 1999) to feed into the northward Intermediate Western Boundary Current and southward Brazil Current (Fig. 6, top).

At both latitudes (34 and 33°S) the transport of the Benguela Current is 2.3 Sv with a standard deviation of about 2 Sv and a shear-based error of about 1 Sv (not shown). This transport is, within the margin of error, consistent with the eastward transport in the South Atlantic Current (0.7 Sv at 14°E) and the westward transport of the Benguela Current Extension (1.3 Sv at 14°E, Figs. 10 and 8a, b).

c. Flow along the western boundary

Profiling floats are not the best instruments to measure boundary currents. Therefore, the flow along the western boundary is quite poorly resolved at several latitudes due to a lack of float observations (Fig. 1 and 6). In the following we analyze the transports based on estimates at latitudes with sufficient observations. The estimated mean northward transport of the Intermediate Western Boundary Current (28 to 6°S) is 2.8 Sv (Fig. 9c). Farther north, the transport of the North Brazil Current (5°S to 5°N) is 3.3 Sv. This northward flow along the western boundary can also be seen in the salinity field (Fig. 3). North of the Benguela Current Extension a tongue of relatively low salinity (less than 34.4 psu) extends from 25°S to the north along the western boundary, in the region of the Intermediate Western Boundary Current and the North Brazil Current. The exception is the region between about 10°S and the equator (see section 3).

Adding the transport of the Intermediate Western Boundary Current just north of the latitude where the Benguela Current Extension reaches the western boundary (2.2 Sv at 27°S) to the mean southward transport of the Brazil Current (5.2 Sv, Fig. 9c) results in 7.4 Sv. This transport corresponds well to the westward transport of the Benguela Current Extension (7.6 Sv at 45°W, Fig. 10). Therefore, within the uncertainties of these transport estimates, two-thirds of the water reaching the western boundary recirculate in the subtropical gyre. This indicates that the bifurcation is more balanced

than an earlier study by Schmid et al. (2000) suggested. In that study, it was found that three quarters of the water reaching the western boundary at intermediate depth recirculates and only one quarter goes northward. The reasons for the difference between these two estimates are likely to be due to the much larger amount of data available for the new estimate and a time dependence of the flow.

Rodrigues et al. (2007) used a reduced gravity primitive equation model to investigate the mean and the seasonal variability of the bifurcation, and found that in the annual mean the bifurcation occurs between 10 to 14°S near the surface and shifts poleward with increasing depth to reach 27°S at 1000 m depth (their Fig. 3, not shown). For the 500 to 1000 m layer Rodrigues et al. (2007) reported that the bifurcation is at its southernmost location in July and at its northernmost location in October, and that the distance between the maximum and the minimum latitude is about 1° (their Fig. 8, not shown). Therefore, at 1000 m, the bifurcation would move back and forth between 27.5 and 26.5°S. In the mean the results from this paper are very similar to those from the model study by Rodrigues et al. (2007). Since the data density in this region is insufficient the seasonality can not be studied based on the observations. Therefore, it remains to be seen if the variability in the model reflects the reality.

d. Intermediate depth contribution to the Meridional Overturning Circulation

An attempt to estimate the zonally integrated meridional transport from the velocity field is made to derive the contribution of the flow at intermediate depth to the Meridional Overturning Circulation. This estimation was possible at many latitudes which fulfilled the requirements of basin-wide observations. The range of derived northward transports extends from 0.8 Sv to 5.7 Sv (Fig. 9d). The average and median derived from all northward transports are 3.3 Sv and 3.5 Sv, respectively. The difference between these two values is quite small, when compared to the uncertainties reflected by the standard deviations and the geostrophic shear (Fig. 9d). Therefore, a meridional transport of about 3 Sv is a robust estimate of the intermediate depth transport contributing to the total northward transport of the Meridional Overturning Circulation. To find out how much the intermediate depth transport contributes to the Meridional Overturning Circulation we compare estimates obtained at 35°S, where we find a northward transport in the 800 to 1100 dbar layer is 2.8 Sv. Dong et al. (2009) estimated the northward transport of the Meridional Overturning Circulation as about 18 Sv at this latitude, and derived 2 Sv in the layer used herein (Dong, personal communication). Therefore, the flow at intermediate depth contributes 11 to 16% to the total transport of the Meridional Overturning Circulation at 35°S.

e. Zonal flows North of the Subtropical Gyre

Between 25°S and 5°S the zonal flow is relatively weak and variable (Fig. 6). However, latitudinally alternating eastward and westward flow is observed. Eastward flow is predominant in the band extending from 19 to 21°S (depending on the longitude), at 10°S and at 6°S, whereas westward flow dominates from 16 to 11°S in the center of the basin, and at 8°S west of 5°W. The fact that some of these flows are not visible in the eastern region may be partly due to insufficient observations for obtaining robust means. The flow between 16 to 11°S is interesting, because it is northwestward and because there are signs that it is fed by a current going north from the Benguela Current before turning northwesterly. The bands of eastward flow around 20 and 6°S coincide with eastward penetrations of relatively fresh AAIW (Fig. 3). In the western part of the Atlantic the transports for these two currents are 1.4 Sv (20.5 to 18.5°S) and 0.5 Sv (6.5 to 5.5°S, Fig. 8c), with standard deviations of more than 1 Sv. Schmid et al. (2003) also reported the predominance of eastward spreading of the AAIW at 6.5 to 5.5°S, with a standard deviation that is more than twice as large as the mean. Since both studies observed mean eastward flow of the same magnitude at this latitude it can be concluded that the mean eastward transport of 0.5 Sv is a robust result.

A westward tongue of relatively salty AAIW is observed between 8 and 12°S (Fig. 3), in a latitude range where the flow is predominantly westward (Fig. 6), with the exception of weak eastward flow at 10°S. Because the eastward flow at 6°S gives rise to a tongue of low salinity the westward tongue of high salinity farther south is more prominent. It needs to be noted that the mean zonal velocity at 10°S is only poorly resolved, with less than 6 floats in two-thirds of the boxes used for the transport estimates (Fig. 1, bottom). In contrast to this more than three-quarters of the boxes used for the transport estimates at 6°S have at least 6 floats in them. Therefore, additional observations at 10°S may yield a different mean flow in the future.

Closer to the equator, at latitudes of 2°, the Northern and Southern Intermediate Countercurrents are well resolved, with eastward transports of 1.3 Sv and 2.0 Sv, respectively (Fig. 8c). The Southern Intermediate Countercurrent can also be seen in the hydrographic field as an eastward penetration of water with a salinity of less than 34.475 psu (Fig. 3). What was uncertain to date is the fate of this current as it approaches the eastern boundary. It has been proposed that the current splits up into a northward branch that merges into the equatorial flow and southward branch (e.g. Stramma and Schott, 1999). Such a flow pattern is not consistent with the salinity field near the equator. While it could be that this is due to a change of the mean flow field over time, it seems more likely that the improved data coverage allows a better determination of the mean pathways along which the AAIW spreads. Based on the new observations in this region it is found that the isoline for 34.5 psu is very close to the equator from the western boundary to 5°W and then tilts southward to end up at

2°S near 5°E. This tilt indicates that relatively fresh water flowing east in the Southern Intermediate Countercurrent does not spread northward near the eastern boundary, contrary to what was proposed earlier. Instead, the new results indicate that, on average, the eastward flow of the Southern Intermediate Countercurrent weakens significantly near the Greenwich Meridian, which allows a southward spreading of more salty equatorial water (salinity larger than 34.5 psu) near the eastern boundary. The fact that this saltier water is found north of 2°S and south of 4°S suggests that a southward flow originating from the equatorial current frequently crosses this area of slightly fresher water supplied by the Southern Intermediate Countercurrent. This could occur at times when the eastward Southern Intermediate Countercurrent does not cross the Greenwich Meridian. Based on results by Schmid et al. (2003), the probability for this is larger in the first half of the year, when the equatorial flow at intermediate depths is to the east and the Southern Intermediate Countercurrent is relatively weak.

5 Variability of the Confluence of the Brazil and Malvinas Current at intermediate depth

As described in section 4a. the Malvinas Current and the Brazil Current meet at 38°S in the 800 to 1100 dbar layer (Fig. 6), which is the average latitude where the retroflection of the Malvinas Current is observed at the surface (e.g. Olson et al., 1988; Garzoli and Garraffo, 1989). This latitude coincides with the latitude where the salinity isoline of 34.1 psu, which separates fresher AAIW from AAIW that recirculated around the subtropical gyre, intersects the western boundary (Fig. 3). An interesting question in this region is whether the variability of the latitude of the Confluence at intermediate depth (800-1100 dbar) is similar to the variability observed at the surface. Up to date the available data were insufficient to address this question.

Currently, the data coverage is not sufficient to determine the variability of the confluence from monthly climatological fields, but quarterly climatological fields indicate that the separation of the subsurface Brazil Current from the continental shelf in the 800 to 1100 dbar layer reaches its northernmost position, about 36°S, during the third quarter (July to September) and is at its southernmost position, about 38°S, in the other quarters (Fig. 11). This seasonality, while relatively poorly resolved, is similar to that at the surface (Goni and Wainer, 2001; Goni et al., 2009).

A comparison with quarterly means of years 11-15 of a high-resolution run of the HYCOM model is used to further analyze the variability of the confluence at the AAIW level. The Isopycnic layer 19 of the HYCOM model is closest to the depth of the floats in this region, as indicated by a map of the layer depth. This layer is at a similar depth as the floats within the Brazil Current and about 100 m shallower in the Malvinas Current (Fig. 12). The model confirms that the latitude of the separation of the Brazil Current from the continental shelf undergoes a seasonal cycle, which corresponds to

changes of the latitudes where the three isolines depicting depths of 750, 870 and 1000 m turn east and separate from the shelf break. This occurs farthest north (between 36.5 and 37.5°S) in the third quarter (Fig. 12, bottom left panel). In the first two quarters (Fig. 12, top panels) the depths contours show that the Malvinas Current retroflects at about 37.5°S, which is within 0.5° of the separation of the Brazil Current in the observed velocity fields. The fourth quarter depicts a situation in between the two extremes (Fig. 12, bottom right panel). This distinction is currently not possible in the observed velocity fields.

6 Conclusions

The results obtained in this paper demonstrated the unique contribution of Argo data to studies of the circulation in the ocean. The availability of simultaneous observations of velocity at 800 to 1100 dbar, as well as salinity and pressure fields at the depth of the AAIW not only allowed the verification of the main features of the AAIW circulation but also showed new and interesting features. From the joint analysis of these data sets a schematic of the intermediate depth flow field can be derived (Fig. 13).

The mean flow field in the subtropical region does not differ much from the flow field observed in earlier studies (e.g. Reid, 1989; Talley, 1996; Boebel et al., 1999; You, 1999; Schmid et al., 2000; Núñez-Riboni et al., 2005). This region is dominated by the anticyclonic circulation around the subtropical gyre that is fed by the Malvinas Current in the southwest and the leakage of the Agulhas Current in the southeast. Some differences are observed in the interaction of the South Atlantic Current and Antarctic Circumpolar Current. For example, Boebel et al. (1999) concluded from Lagrangian observations that the South Atlantic Current shifts southward on the way to the east (to almost 45°S at 10°W) and that some water from the Antarctic Circumpolar Current splits off to the north and joins the South Atlantic Current east of 35°W. Our results indicate that the South Atlantic Current is always north of 40°S, and that some water leaves it towards the south at about 30°W to join the Antarctic Circumpolar Current. Núñez-Riboni et al. (2005) show a flow field that is closer to the one found herein, but as in the study by Boebel et al. (1999), there were insufficient data to resolve the flow field of the South Atlantic Current and Antarctic Circumpolar Current. Another difference to earlier depictions of the subtropical gyre is that the new results show that the Benguela Current Extension feeds into the Intermediate Western Boundary Current following two pathways. One pathway is directly to the west, while the other pathway carries water that is deflected to the north near 35°W and joins the Intermediate Western Boundary Current just south of 20°S as indicated in Figure 13.

A detailed analysis of the flow in the eastern part of the study region clearly indicates that the Agulhas Current enters the Atlantic south of Africa and retroflects between 16 and 20°E, while the Agulhas leakage feeds into the Benguela Current (Fig. 13), which is in agreement with earlier results

(e.g. Lutjeharms and van Ballegooyen, 1988). East of 13°E, this current bifurcates into two branches: the Benguela Current Extension and a northwestward flow entering the interior basin at about 20°S. Some indications for the existence of this flow were found in hydrographic observations (You, 1999) but they were never verified by directly observed velocities (e.g. Boebel et al., 1999; Schmid et al., 2000; Núñez-Riboni et al., 2005). The fate of this current west of 25°W cannot be determined from the new velocity field (Fig. 6). According to You (1999) it joins the western boundary current north of 10°S, which is not supported by the velocity field in Figure 6, mainly because of the weak eastward flow at 10°S. More observations are needed to find out how robust the westward current is and where it reaches the western boundary. In addition, the new observations indicate the potential existence of another band that is fed by water coming from the Benguela Current. It is located between the Benguela Current Extension and a band of eastward flow near 20°S and has weak westward flow that reaches the western boundary (dashed line in Fig. 13).

The new estimates of the transport of the South Atlantic Current show a variability with longitude that was not previously observed. The transport decreases from about 5-10 Sv in the west to about 1 Sv in the east with an almost linear trend (Fig. 10). In an earlier study, some variability was observed in the western side of the basin, where the transport decreased from 11 to 5 Sv between 38 and 28°W (Schmid et al., 2000)[6]. The longitude-dependence of the transport of the South Atlantic Current could be explained by northward outflow of water in the South Atlantic Current, as indicated by significant northward transports in the interior of the subtropical gyre, e.g., about 3 Sv near the Greenwich Meridian, Fig. 9a).

Another conclusion from the current analysis is that the transport of the Benguela Current Extension also depends on the longitude. It increases almost linearly from about 1 Sv in the east to about 8 Sv in the west (Fig. 10). Transport estimates by Schmid et al. (2000) resulted in a mean westward transports of 13 Sv for the flow between 20 and about 34-36°S for longitudes between 30 and 40°W, which was a region of westward flow in their data set. This latitude range is larger than the latitude range used herein. The difference in the approach is due to the fact that the added data allow a separation between the Benguela Current Extension and the flow to the north. This northern band of weak westward flow (dashed line in Fig. 13) is also fed by the Benguela Current, but is interspersed with a large number of eastward velocity vectors (Fig. 6). The transport of 13 Sv derived by Schmid et al. (2000) is just outside the range of adjusted transports[6] of about 8 to 11 Sv found for 24.5 to 33.5-35.5°S (Fig. 10). This difference seems insignificant because the different width of the currents assumed for the calculation, about 15° versus about 10°, results in a difference of the transports by a factor of 1.5. Dividing the 13 Sv derived by Schmid et al. (2000) by 1.5 results in 8.7 Sv, which is

[6]In Schmid et al. (2000) a 500 m thick layer was used. Their estimates were made comparable with the transports in a 300 m layer by multiplication with 0.6.

within the range of adjusted values (8 to 11 Sv) derived here.

In a study by Núñez-Riboni et al. (2005) only the zonal means for the transports in the South Atlantic Current and the Benguela Current Extension were derived as 8.5±3.5 Sv and 9.3±3.4 Sv, respectively. A direct comparison of these transports with the new estimates is not possible, because Núñez-Riboni et al. (2005) used the neutral density surfaces 27.25 and 27.55 $kg\,m^{-3}$ as the boundaries of the AAIW layer, which means the thickness of this isoneutral layer depends on the latitude and longitude. In most regions, the isoneutral layer will be thicker than the layer used herein. If we assume that the thickness of the isoneutral layer is about 500 m, then we can use the same approach as before to make them comparable[6]. This approach results in 5.1 Sv and 5.6 Sv for the adjusted transports of their estimates for the South Atlantic Current and the Benguela Current Extension, respectively. The adjusted transports are similar to the newly estimated transports in the western part of the basin.

In the region of the Santos bifurcation, the Benguela Current Extension splits up and feeds into the northward Intermediate Western Boundary Current and the southward Brazil Current (Fig. 13). The mean bifurcation latitude is found to be at about 28.5°S (Fig. 6). In an earlier study of the mean spreading of the Antarctic Intermediate Water by Boebel et al. (1999) the bifurcation was reported to be at 28°S, which agrees with our result within the margin of error. Model results by Rodrigues et al. (2007) are in general agreement with the observations. In that study the mean location of the bifurcation is found at 27°S in 1000 m depth. An interesting question is how much of the transport into the bifurcation region goes south and how much goes north. It is observed that the mean southward transport in the Brazil Current is about 5.2 Sv (Fig. 9c) and the mean northward transport in the Intermediate Western Boundary Current is about 2.2 Sv just north of the bifurcation (Fig. 9c). The sum of these two transports is 7.4 Sv, which corresponds well with the transport of 7.6 Sv of the Benguela Current Extension near the western boundary, at 45°W. Therefore, it can be concluded that two-thirds of the water entering the bifurcation region recirculates in the subtropical gyre. Schmid et al. (2000) found that three-quarters of the water reaching the western boundary at intermediate depth recirculates and only one quarter goes northward. Núñez-Riboni et al. (2005) show the transports along the western boundary in their Figure 4.15. From that figure we determined that their estimate of the mean transport in the Brazil Current is about 4 Sv, and that their estimate for the transport of the Intermediate Western Boundary Current just north of the bifurcation is about 1 Sv. Therefore, their study indicates that about 80% of the water recirculates in the subtropical gyre. A comparison of their result, as determined from their figure, and the result by Schmid et al. (2000) yields a difference of only 5%, which can be seen as insignificant within the uncertainty of the method. It seems likely that the difference between the two earlier estimates and our new estimate (about 10% to 15%) are due to a combination of temporal variability and the much larger amount of observations available now.

The confluence of the Malvinas and Brazil Current is observed near 38°S between 800 and 1100 dbar (Fig. 6) and shown schematically in Figure 13. In addition to the mean location, the velocity observations reveal a seasonal variability of the location of the confluence of the Brazil Current and Malvinas Current at intermediate depths, with the separation of the Brazil Current from the boundary at 36°S in the third quarter and at 38°S in the other three quarters. This variability is similar to that observed at the surface (Goni and Wainer, 2001; Goni et al., 2009). In the HYCOM model the separation of the Brazil Current occurs farthest north (between 36.5 and 37.5°S) and the Malvinas Current penetrates farthest to the north in the third quarter, which is consistent with the observations. The confluence is at its southernmost location in the first two quarters and in between the two extremes in the fourth quarter. This distinction cannot be made from the observed velocity field due to a lack of data.

While the zonal flow between 25°S and 5°S is relatively weak and variable (Fig. 6), it is observed that eastward flow is predominant at 19 to 21°S (depending on the longitude), at 10°S and at 6°S, whereas westward flow dominates from 16 to 11°S in the center of the basin, and at 8°S west of 5°W. The northwestward flow between 16 to 11°S is fed by a current going north from the Benguela Current (Fig. 13). The bands of eastward flow around 20-19°S and 6°S coincide with eastward penetrations of relatively fresh AAIW (Fig. 3). Their transports in the western part of the Atlantic are 1.4 Sv (20.5 to 18.5°S) and 0.5 Sv (6.5 to 5.5°S), respectively (Fig. 8c). Schmid et al. (2003) also reported the presence of an eastward current (the South Equatorial Countercurrent) at 6°S, which indicates that this current is quite stable.

A westward tongue of relatively salty AAIW is observed between 8 and 12°S (Fig. 3), in a latitude range where the flow is predominantly westward (Fig. 6). The only exception is the eastward flow at 10°S. However, it needs to be noted that the mean zonal velocity at 10°S is only poorly resolved. Therefore, it seems possible that additional observations at 10°S could yield a mean flow consistent with the observed salinity distribution in the future.

The new data set confirms previous results regarding the location of the major zonal currents near the equator (e.g. Schmid et al., 2001; Schmid et al., 2003; Ollitrault et al., 2006), but there now are more data in the eastern Tropical Atlantic. The strong eastward Northern Intermediate Countercurrent and Southern Intermediate Countercurrent are present at latitudes of about 2° on both sides of the equator. New is that there are indications for southward spreading of AAIW from the equator near the eastern boundary (Fig. 3). However, currently the only sign for this can be found in the salinity distribution (Fig. 3). It also seems likely, that the Northern Intermediate Countercurrent does not penetrate as far east as suggested by Stramma and Schott (1999). Instead there are signs of eastward flow into the Gulf of Guinea that are fed by eastward flow from a current found at about 5°N in the western part of the Atlantic. It remains to be seen how robust this flow is. Consistent with the theory

of the ventilated thermocline (Luyten et al., 1983) a shadow zone (indicate by an S in Fig. 13) exists in the eastern tropical Atlantic, south of the equator. This zone is characterized by relatively salty AAIW (Fig. 3) and is located in the region of the Angola Gyre.

The basin-wide meridional transport in the 800 to 1100 dbar layer (which is part of the Meridional Overturning Circulation), based on all positive transports shown in Figure 9d, is about 3.5 Sv. Our estimate of 2.8 Sv at 35°S amounts to about 16% of the 18 Sv Dong et al. (2009) derived for the total the northward transport of the Meridional Overturning Circulation at this latitude. For the intermediate depth layer used herein they derived 2 Sv (Dong, personal communication), which compares well with our result. The comparison with the total northward transport of the Meridional Overturning Circulation indicates that the northward transport of Antarctic Intermediate Water contributes significantly to it because: (1) the layer thickness used herein amounts to about 23% of the thickness of the layer occupied by the upper branch of the Meridional Overturning Circulation in the South Atlantic, which is close to the 16% contributed by the transport of AAIW; and (2) because the Ekman transport, which is also seen as a significant contribution to the Meridional Overturning Circulation, amounts to a smaller percentage (9%) of the total transport of the Meridional Overturning Circulation (Dong et al., 2009).

Acknowledgements

We want to thank everybody involved in the Argo project for their contributions to generating a high-quality global sub-surface data set. We want to thank Zulema Garraffo and E. Joseph Metzger for providing the HYCOM output. We want to thank National Center for Environmental Prediction (NCEP) for providing the data from the Global Ocean Data Assimilation System (GODAS) model, and National Oceanographic Data Center (NODC) for providing the World Ocean Atlas 2005.

References

Antonov, J. I., R. A. Locarnini, T. P. Boyer, A. V. Mishonov, and H. E. Garcia. 2006. World Ocean Atlas 2005, Volume 2: Salinity. S. Levitus, Ed. NOAA Atlas NESDIS 62, U.S. Government Printing Office, Washington, D.C.

Belkin, I. M. and A. L. Gordon. 1996. Southern Ocean Fronts from the Greenwich Meridian to Tasmania. J. Geophys. Res. *101*, 3675–3696.

Bleck, R. 2009. An oceanic general circulation model framed in hybrid isopycnic-Cartesian coordinates. Ocean Model *4*, 55–88.

Boebel, O., R. E. Davis, M. Ollitrault, R. G. Peterson, P. L. Richardson, C. Schmid, and W. Zenk. 1999. The intermediate depth circulation of the Western South Atlantic. Geophys. Res. Lett. *26*, 3329–3332.

Boebel, O., T. Rossby, J. R. E. Lutjeharms, W. Zenk, and C. Barron. 2003. Path and variability of the Agulhas Return Current. Deep-Sea Res. II *50*, 35–56.

Carnes, M. R. 2003. Description and evaluation of GDEM-v3.0. Naval Oceanograpic Office Technical Note, 28 pp.

Chassignet, E., L. Smith, G. Halliwell, and R. Bleck. 2003. North Atlantic simulations with the hybrid coordinate ocean model (HYCOM): impact of the vertical coordinate choice, reference density, and thermobaricity. J. Phys. Oceanogr. *34*, 2504–2526.

Davis, R. E., P. D. Killworth, and J. L. Blundell. 1996. Comparison of Autonomous Lagrangian Circulation Explorer and Fine Resolution Antarctic Model results in the South Atlantic. J. Geophys. Res. *101*, 855–884.

Deacon, G. E. R. 1933. A general account of the hydrology of the South Atlantic Ocean. Discovery Reports *7*, 171–238. Cambridge University Press.

Defant, A. 1941. Quantitative Untersuchungen zur Statik und Dynamik des Atlantischen Ozeans. Wiss. Ergebnisse dtsch. atlant. Exped. "METEOR", 6(2), 191-260.

Dong, S., S. L. Garzoli, M. O. Baringer, C. S. Meinen, , and G. J. Goni. 2009. The Atlantic Meridional Overturning Circulation and its Northward Heat Transport in the South Atlantic. Geophys. Res. Lett. *to be submitted*.

Flood, R. D. and A. N. Shor. 1988. Mud waves in the Argentine Basin and their relationship to regional nottom circulation patterns. Deep-Sea Res. *35*, 943–971.

Garzoli, S. L. and A. Bianchi. 1987. Time-space variability of the local dynamics of the Malvinas-Brazil Confluence as revealed by inverted echo sounders. J. Geophys. Res. *92*, 1914–1922.

Garzoli, S. L. and Z. Garraffo. 1989. Transports, frontal motions and eddies at the Brazil-Malvinas currents confluence. Deep-Sea Res. *36*, 681–703.

Garzoli, S. L. and A. L. Gordon. 1996. Origins and variability of the Benguela Current. J. Geophys. Res. *101*, 897–906.

Goni, G. J., F. Bringas, and P. N. DiNezio. 2009. Low Frequency Variability of the Brazil Current Front. JPO, submitted.

Goni, G. J. and I. Wainer. 2001. Brazil Current front dynamics from altimeter data. J. Geophys. Res. *106*, 31,117–31,128.

Gordon, A. L. and K. T. Bosley. 1991. Cyclonic gyre in the tropical South Atlantic. Deep-Sea Res. *38*(suppl.), 323–343.

Gordon, A. L. and L. C. Greengrove. 1986. Geostrophic circulation of the Brazil-Falkland confluence. Deep-Sea Res. *33*), 573–585.

Halliwell, G. R. 2004. Evaluation of vertical coordinate and vertical mixing algorithms in the hybrid-coordinate ocean model (HYCOM). Ocean Modelling *7*, 285–322.

Hiller, W. and R. H. Käse. 1983. Objective Analysis of Hydrographic Data Sets from Mesoscale Surveys. Ber. Inst. Meeresk. Univ. Kiel *116*, 78 pp.

Locarnini, R. A., A. V. Mishonov, J. I. Antonov, T. P. Boyer, and H. E. Garcia. 2006. World Ocean Atlas 2005, Volume 1: Temperature. S. Levitus, Ed. NOAA Atlas NESDIS 61, U.S. Government Printing Office, Washington, D.C.

Lutjeharms, J. R. E. and R. C. van Ballegooyen. 1988. The retroflection of the Agulhas Current. J. Phys. Oceanogr. *18*, 1570–1583.

Luyten, J. R., J. Pedlosky, and H. M. Stommel. 1983. The ventilated thermocline. J. Phys. Oceanogr. *13*, 292–309.

Núñez-Riboni, I., O. Boebel, M. Ollitrault, Y. You, P. L. Richardson, and R. Davis. 2005. Lagrangian circulation of Antarctic Intermediate Water in the subtropical South Atlantic. Deep-Sea Res. *52*, 545–564.

Ollitrault, M., M. Lankhorst, D. Fratantoni, P. Richardson, and W. Zenk. 2006. Zonal intermediate currents in the equatorial Atlantic Ocean. Geophys. Res. Lett. *33*, DOI: 10.1029/2005GL025368.

Olson, D. B., G. P. Podesta, R. H. Evans, and O. B. Brown. 1988. Temporal variations in the seperation of the Brazil and Malvinas Currents. Deep-Sea Res. *35*, 1971–1990.

Orsi, A. H., T. W. W. III, and W. D. Nowlin Jr. 1995. On the meridional extent and fronts of the Antarctic Circumpolar Current. Deep-Sea Res. *42*, 641–673.

Reid, J. L. 1989. On the total geostrophic circulation of the South Atlantic Ocean: Flow patterns, tracers and transports. Progress in Oceanography *23*, 149–244.

Richardson, P. L. and S. L. Garzoli. 2003. Characteristics of intermediate water flow in the Benguela Current as measured with RAFOS floats. Deep-Sea Res. II *50*, 87–118.

Rintoul, S. R. 1991. South Atlantic interbasin exchange. J. Geophys. Res. *96*, 2675–2692.

Rodrigues, R. R., L. M. Rothstein, and M. Wimbush. 2007. Seasonal Variability of the South Equatorial Current Bifurcation in the Atlantic Ocean: A Numerical Study. J. Phys. Oceanogr. *37*, 16–30.

Schmid, C., Z. D. Garraffo, E. Johns, and S. L. Garzoli. 2003. Pathways and Variability at Intermediate Depths in the Tropical Atlantic. Interhemispheric Water Exchange in the Atlantic Ocean, Elsevier Oceanography Series, 68, G. J. Goni and P. Malanotte-Rizzoli, Eds. Elsevier, New York, 233–268.

Schmid, C., R. L. Molinari, and S. L. Garzoli. 2001. New Observations of the Intermediate Depth Circulation in the Tropical Atlantic. J. Mar. Res. *59*, 281–312.

Schmid, C., R. L. Molinari, R. Sabina, Y.-H. Daneshzadeh, X. Xia, E. Forteza, and H. Yang. 2007. The Real-Time Data Management System for Argo Profiling Float Observations. J. Atmos. Oceanic Technol. *24*, 1608–1628, DOI: 10.1175/JTECH2070.1.

Schmid, C., G. Siedler, and W. Zenk. 2000. Dynamics of Intermediate Water Circulation in the Subtropical South Atlantic. J. Phys. Oceanogr. *30*, 3191–3211.

Stramma, L. and F. A. Schott. 1999. The Mean Flow Field of the Tropical Atlantic Ocean. New Views of the Atlantic, W. Zenk, R. G. Peterson, and J. R. E. Lutjeharms, Eds. Deep-Sea Res. II, *46*, 279–303.

Suga, T. and L. D. Talley. 1995. Antarctic Intermediate Water Circulation in the Tropical and Subtropical South Atlantic. J. Geophys. Res. *100*, 13,441–13,453.

Talley, L. D. 1996. Antarctic Intermediate Water in the South Atlantic. The South Atlantic: Present and past circulation, G. Wefer, W. H. Berger, G. Siedler, and D. J. Webb, Eds. Springer Verlag, Berlin Heidelberg, 219–238.

Teague, W. J., M. J. Carron, and P. J. Hogan. 1990. A comparison between the generalized digital environmental model and Levitus climatologies. J. Geophys. Res. *95*, 7167–7183.

Uppala, S., P. Kållberg, A. Simmons, U. Andrae, V. da Costa Bechtold, M. Fiorino, J. Gibson, J. Haseler, A. Hernandez, G. Kelly, X. Li, K. Onogi, S. Saarinen, N. Sokka, R. Allan, E. Andersson, K. Arpe, M. Balmaseda, A. Beljaars, L. van de Berg, J. Bidlot, N. Bormann, S. Caires, F. Chevallier, A. Dethof, M. Dragosavac, M. Fisher, M. Fuentes, S. Hagemann, E. Hólm, B. Hoskins, L. Isaksen, P. Janssen, R. Jenne, A. McNally, J.-F. Mahfouf, J.-J. Morcrette, N. Rayner, R. Saunders,

P. Simon, A. Sterl, K. Trenberth, A. Untch, D. Vasiljevic, P. Viterbo, and J. Woollen. 2005. The ERA-40 re-analysis. Quart. J. Roy. Meteor. Soc. *131*, 2961–3012, DOI: 10.1256/QJ.04.176.

Wüst, G. 1935. Schichtung und Zirkulation des Atlantischen Ozeans. Das Bodenwasser und die Stratosphäre. Wiss. Ergebn. Dt. Atl. Exp. "METEOR" 1925-1927, 6, 1-288, Berlin.

You, Y. 1999. Dianeutral mixing, transformation andtransport of Antarctic Intermediate Water in the South Atlantic. Deep-Sea Res. II *46*, 393–435.

You, Y. 2002. Quantitative estimate of Antarctic Intermediate Water contributions from the drake passage and the southwest Indian Ocean to the south Atlantic. J. Geophys. Res. *107*, 3031, DOI: 10.1029/2001JC000880.

You, Y., J. R. E. Lutjeharms, O. Boebel, and W. P. M. de Ruijter. 2003. Quantification of the inter-ocean exchange of intermediate water masses around South Africa. Deep-Sea Res. II *50*, 197–228.

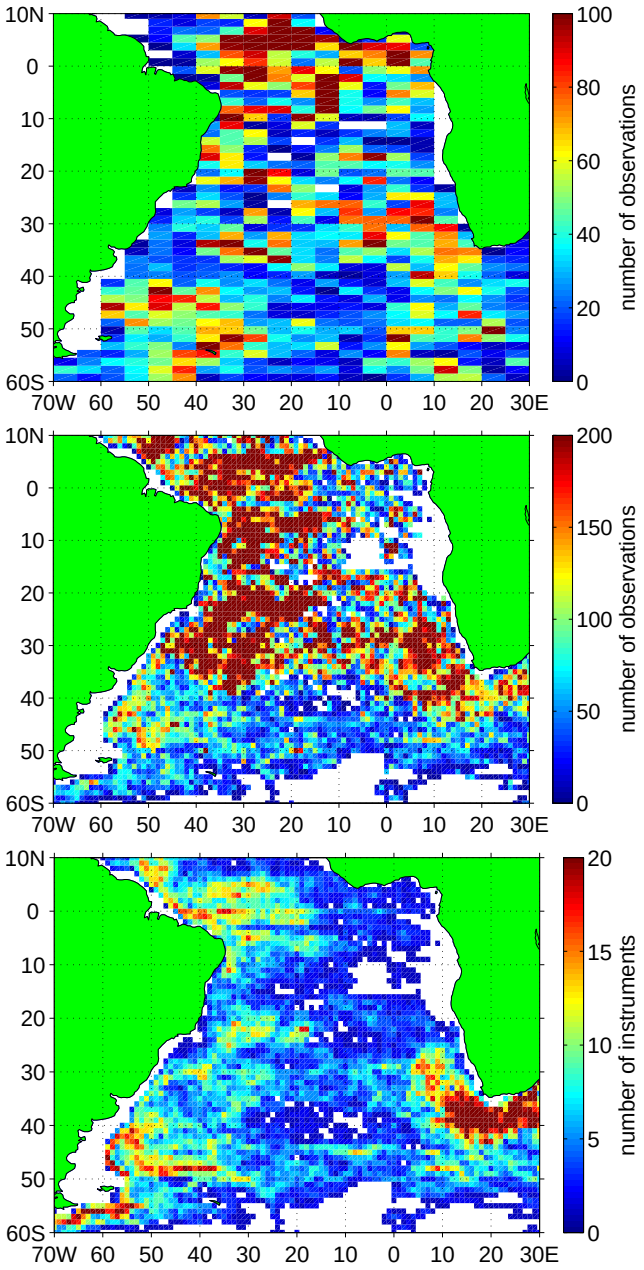

FIG. 1: Top: Data coverage for hydrographic properties based on the profiles collected in January 2006 to December 2008. Dark red indicates 100 observations of the salinity minimum or more. Middle: number of velocity observations in each box (normalized to daily measurements). Dark red indicates 200 observations or more. Bottom: number of floats available for velocity in each box. Dark red indicates 20 floats or more.

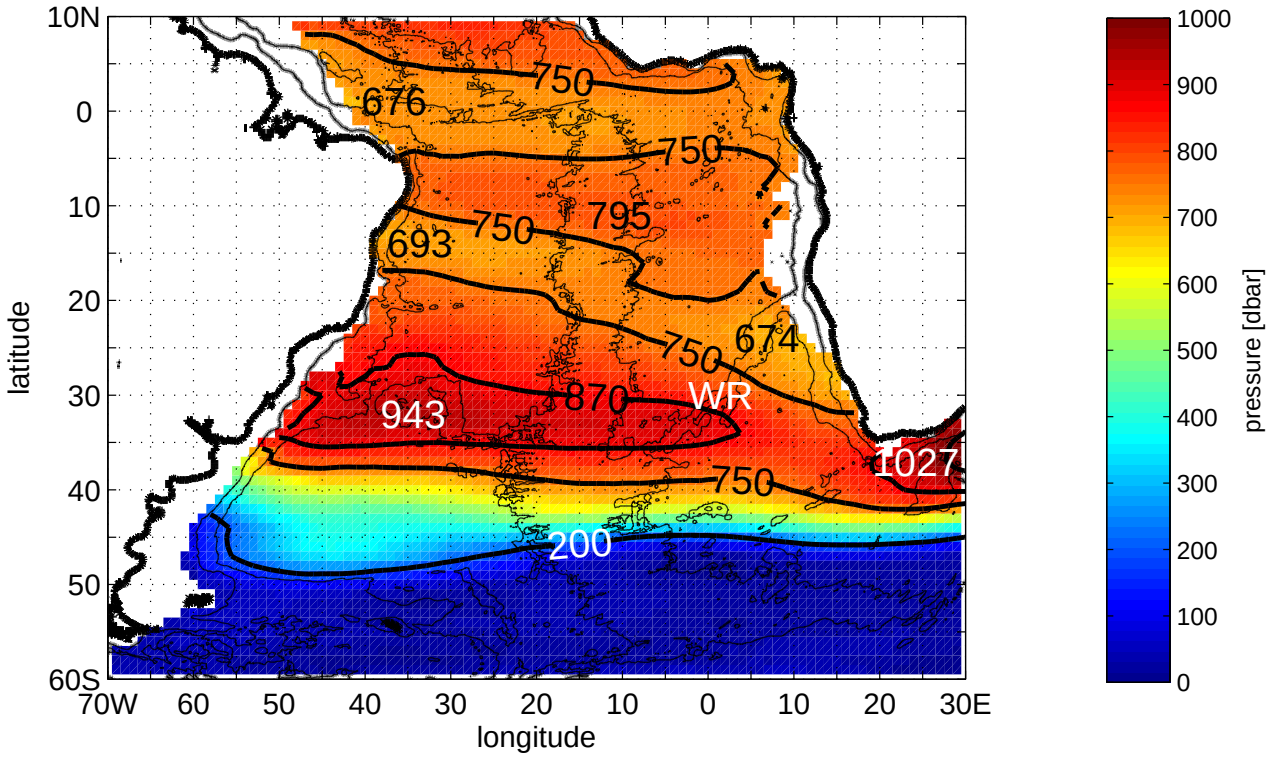

FIG. 2: Climatological mean of the pressure at salinity minimum. Numbers without isolines indicate maxima and minima of the pressure. The 1000 and 4000 m isobath are shown as thin black lines. WR marks the Walvis Ridge.

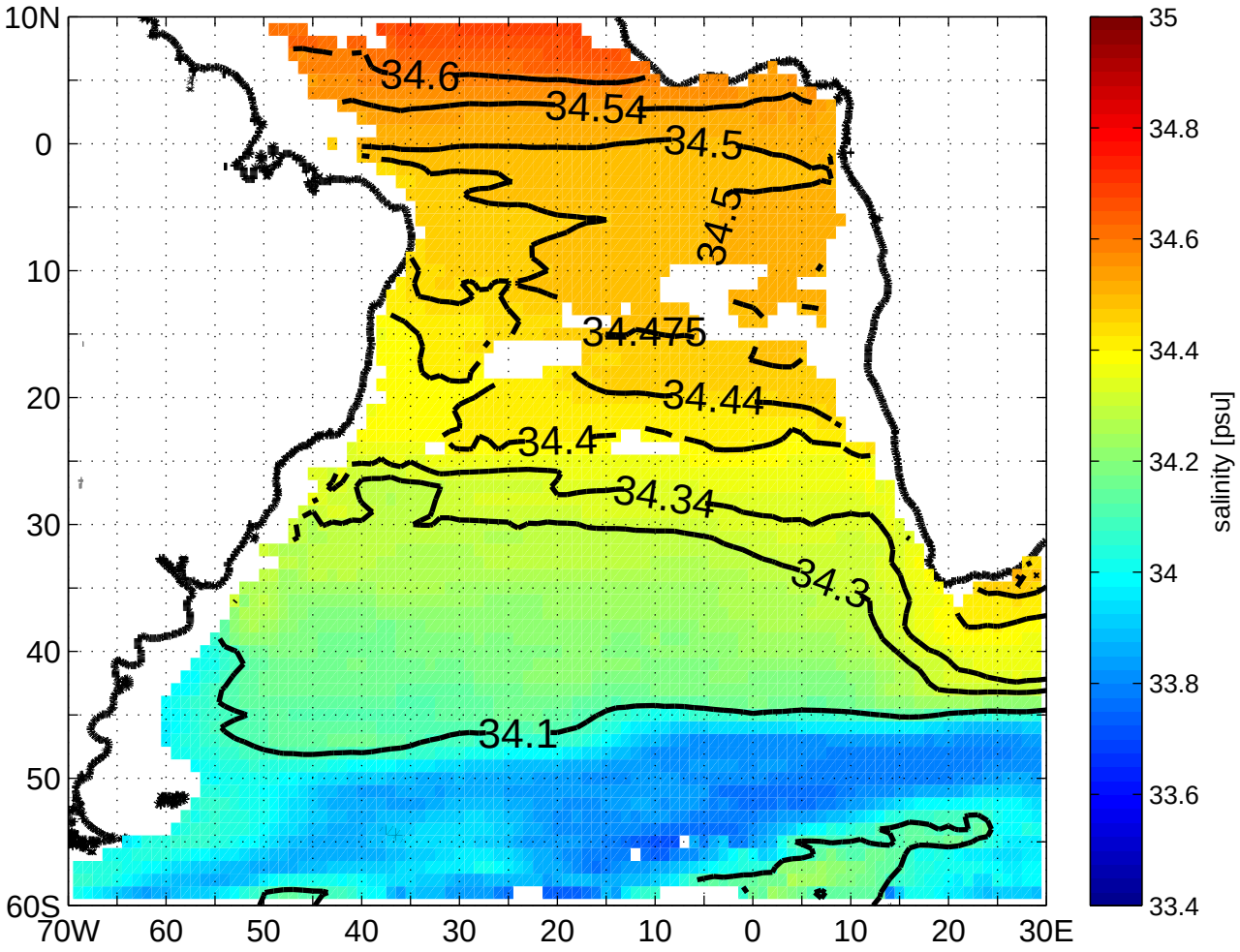

FIG. 3: Climatological mean of the salinity at the salinity minimum.

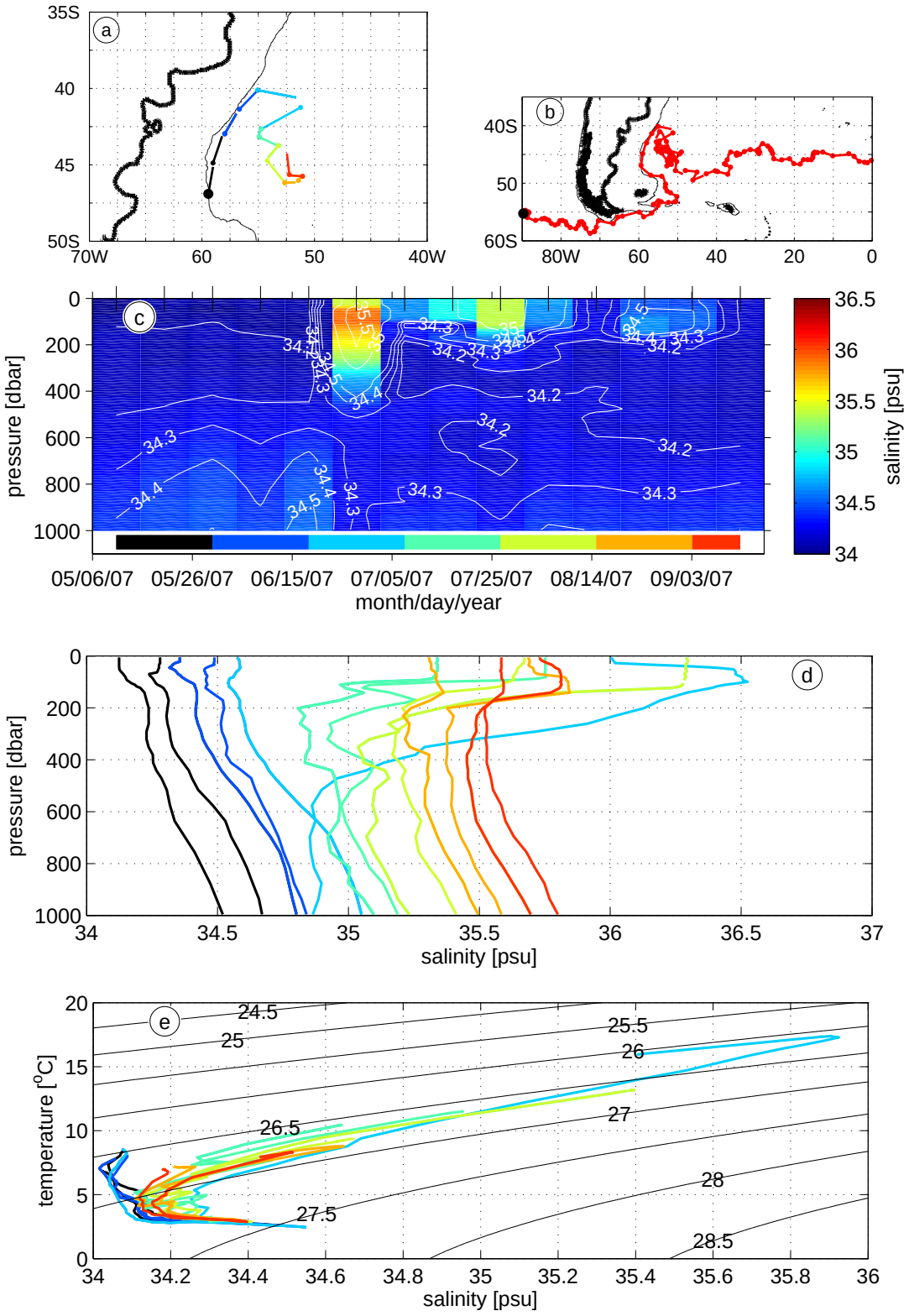

FIG. 4: Partial (a) and complete (b) trajectory, salinity section (c), waterfall plot (d) and T-S diagram with isolines depicting σ_0 (e) for float 3900426. The seven colors (black to red) depict the time. The big black dots in the maps mark the starting point of the shown trajectory. The thin black line in (a) and (b) is the 1000 m isobath.

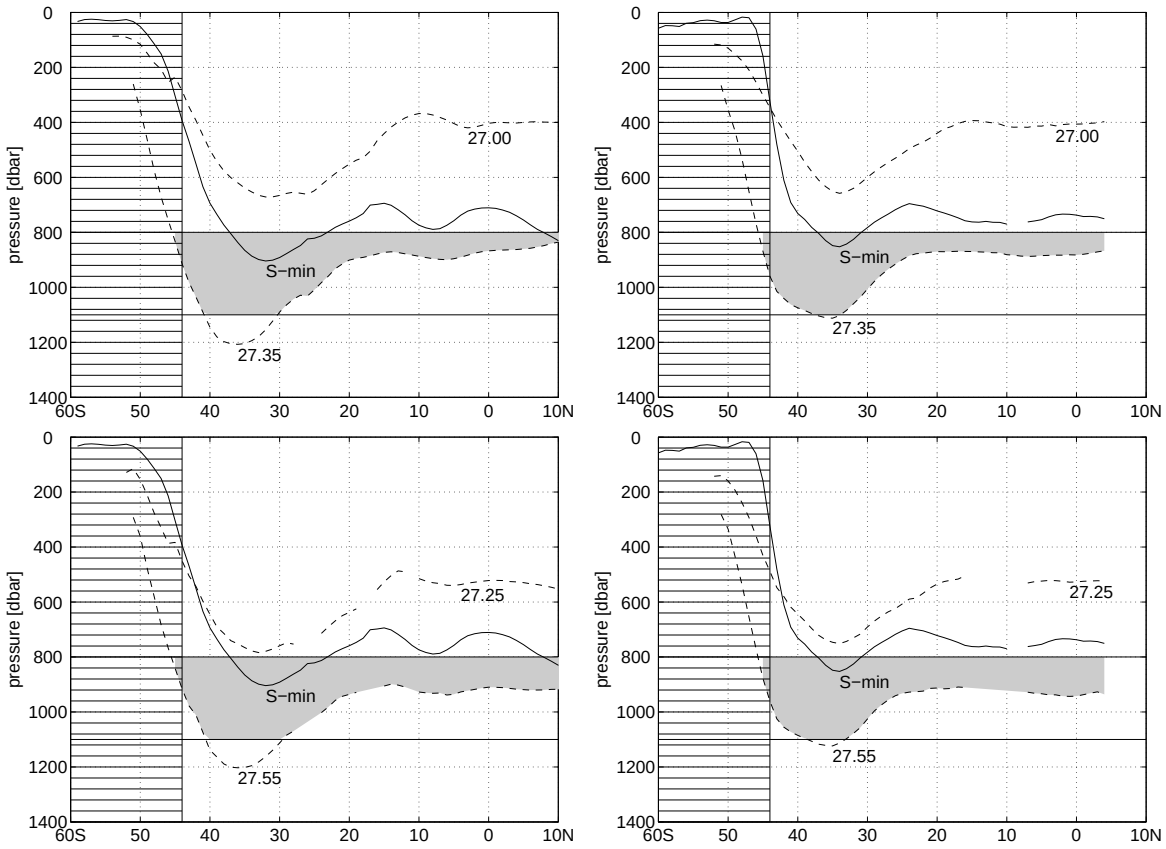

FIG. 5: Meridional transect showing climatological mean of the pressure at the salinity minimum (solid curve) and: the potential density surfaces 27.00 and 27.35 $kg\,m^{-3}$ (top); the neutral density surfaces 27.25 and 27.55 $kg\,m^{-3}$ (bottom). Left: averaged over 20 to 30°W. Right: averaged over 0 to 10°E. The hatched area is south of 44°S. The shaded area indicates the part of the Antarctic Intermediate Water layer, as defined by the selected density surfaces, within 800 to 1100 dbar.

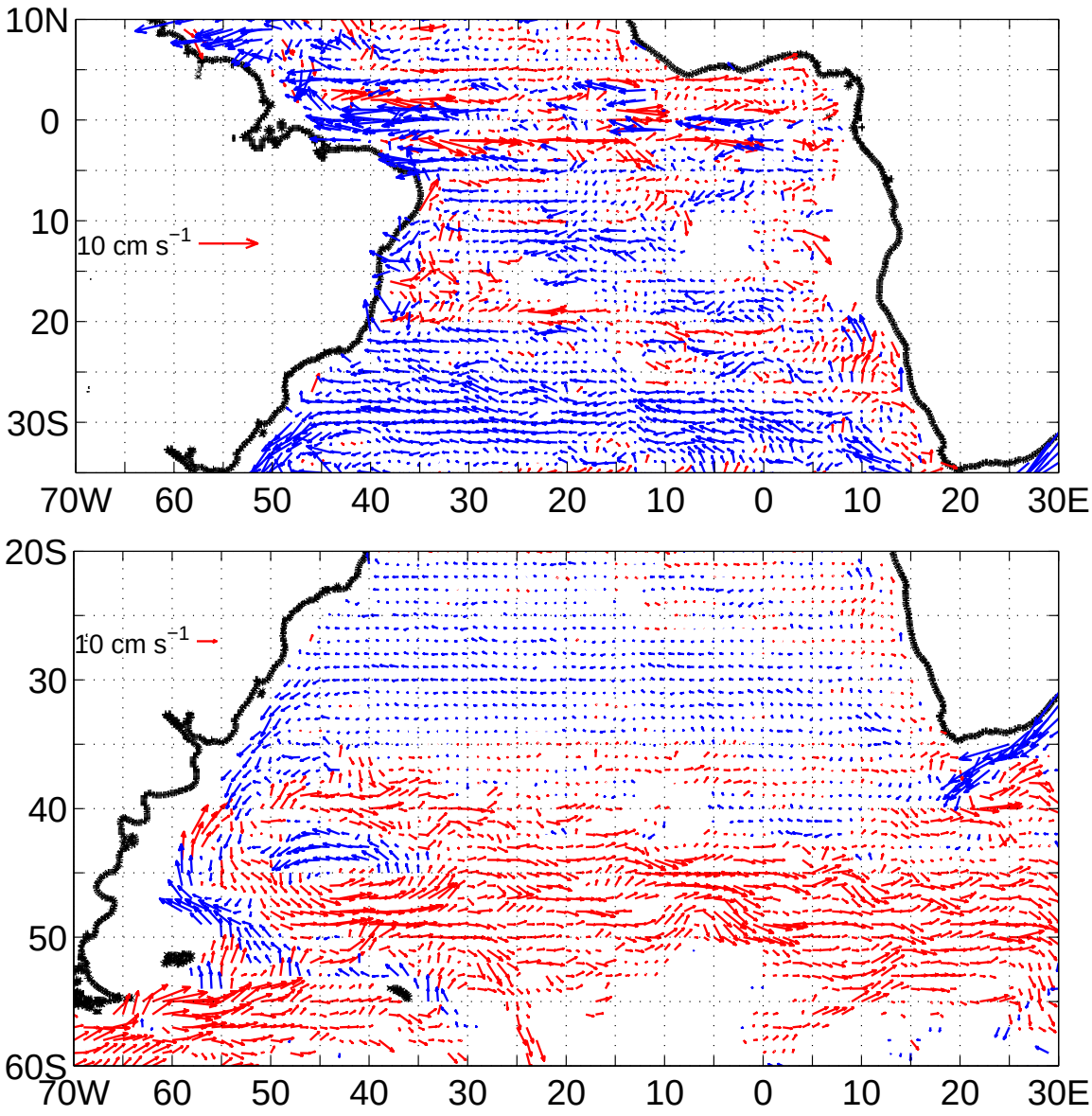

FIG. 6: Annual mean velocity between 800 and 1100 dbar, as derived from objectively mapped quarterly mean fields of the elocities. Red to the east, blue to the west. The upper (lower) panel shows the northern (southern) part of the domain. Note that different scales are used for the vectors in the two panels.

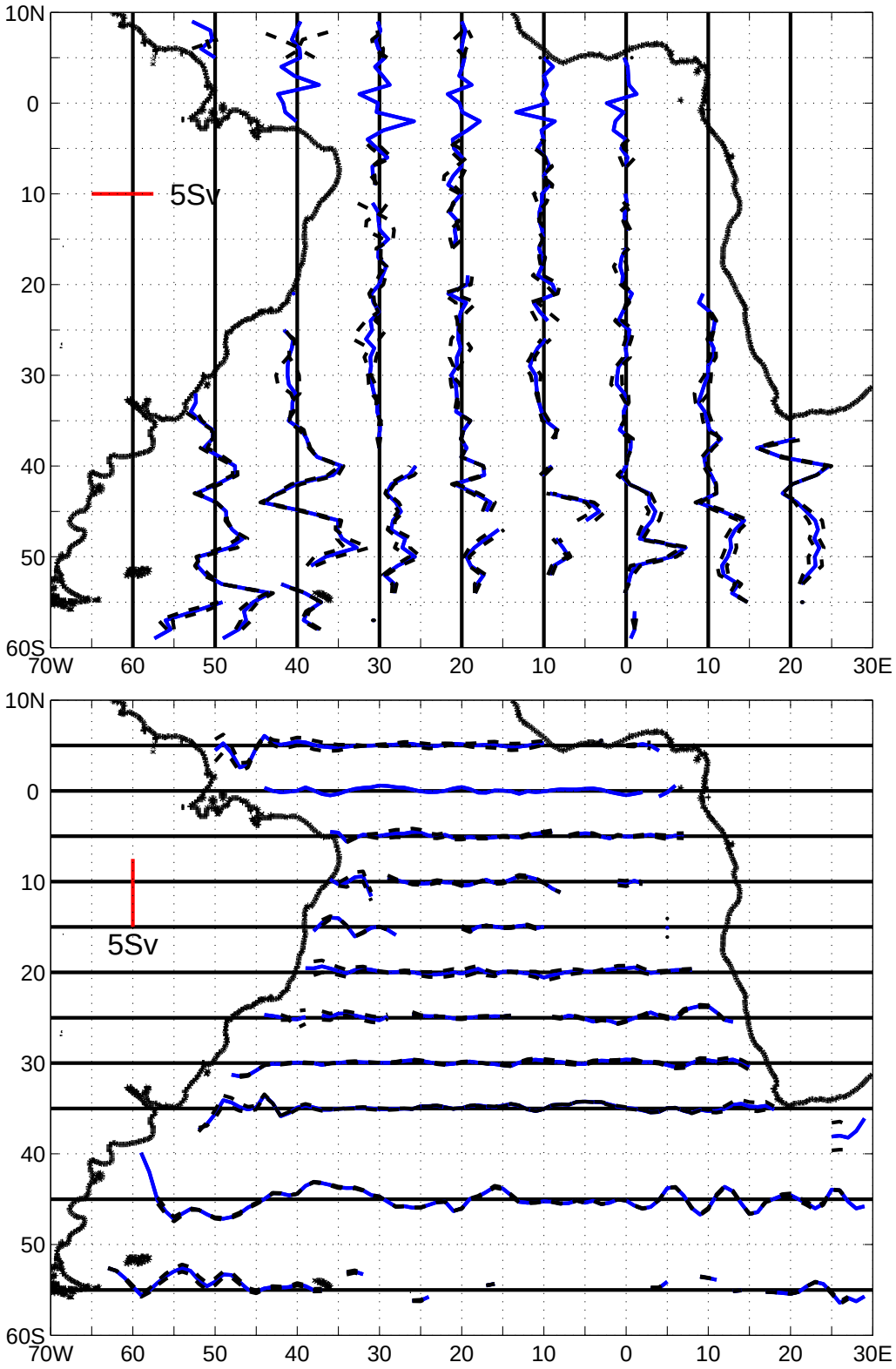

FIG. 7: Annual mean transport between 800 and 1100 dbar (blue lines). The mean was derived from objectively mapped quarterly mean fields of the velocity. The shear-based error is shown by the black dashed lines. Top: zonal. Bottom: meridional.

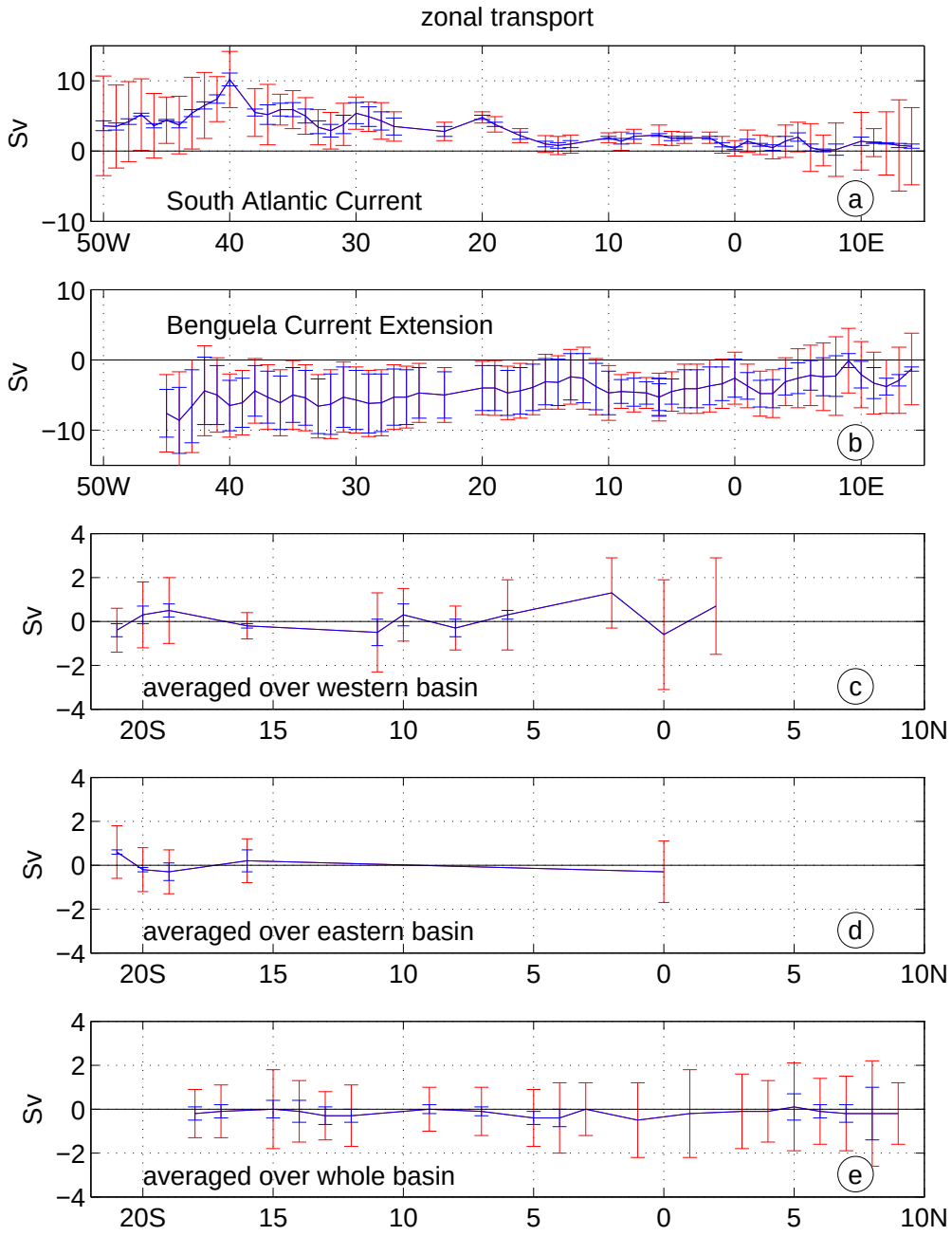

FIG. 8: Annual mean zonal transports between 800 and 1100 dbar derived from objectively mapped quarterly mean fields of the velocity. The red error bars display the total error (standard deviation plus the shear-based error) and the blue error bars represent the shear-based error. (a) South Atlantic Current, (b) Benguela Current Extension, (c) averaged over western basin, (d) averaged over eastern basin, (e) averaged over whole basin.

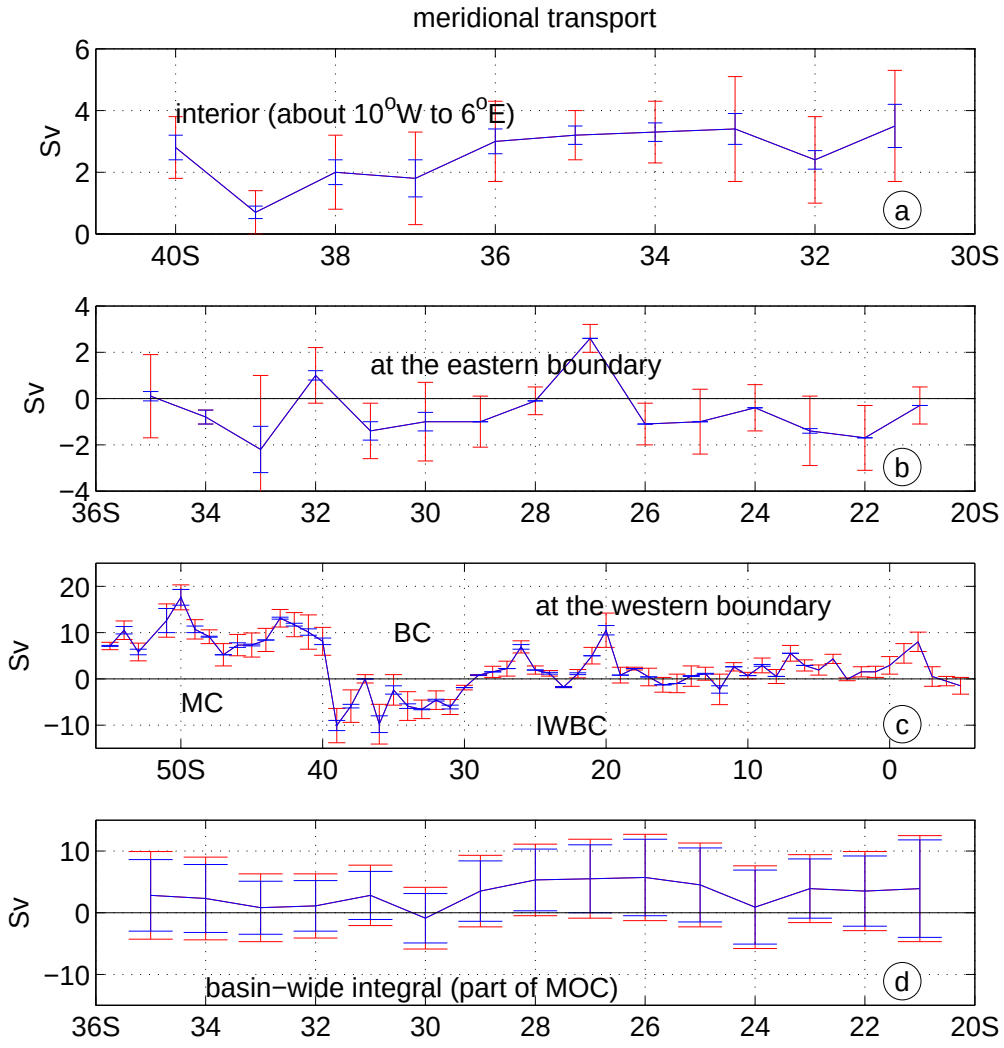

FIG. 9: Annual mean meridional transports between 800 and 1100 dbar, derived from quarterly mean fields of the velocity. The red error bars display the total error (standard deviation plus the shear-based error) and the blue error bars represent the geostrophic shear. (a) interior, (b) at the eastern boundary, (c) at the western boundary, (d) basin-wide integral. The individually marked currents are Malvinas Current (MC), Brazil Current (BC) and Intermediate Western Boundary Current (IWBC). The basin-wide integral represents the contribution of the flow at intermediate depth to the Meridional Overturning Circulation (MOC). Transports in the narrow boundary currents are based on the box-averaged velocities. All other transports are based on the objectively mapped velocities.

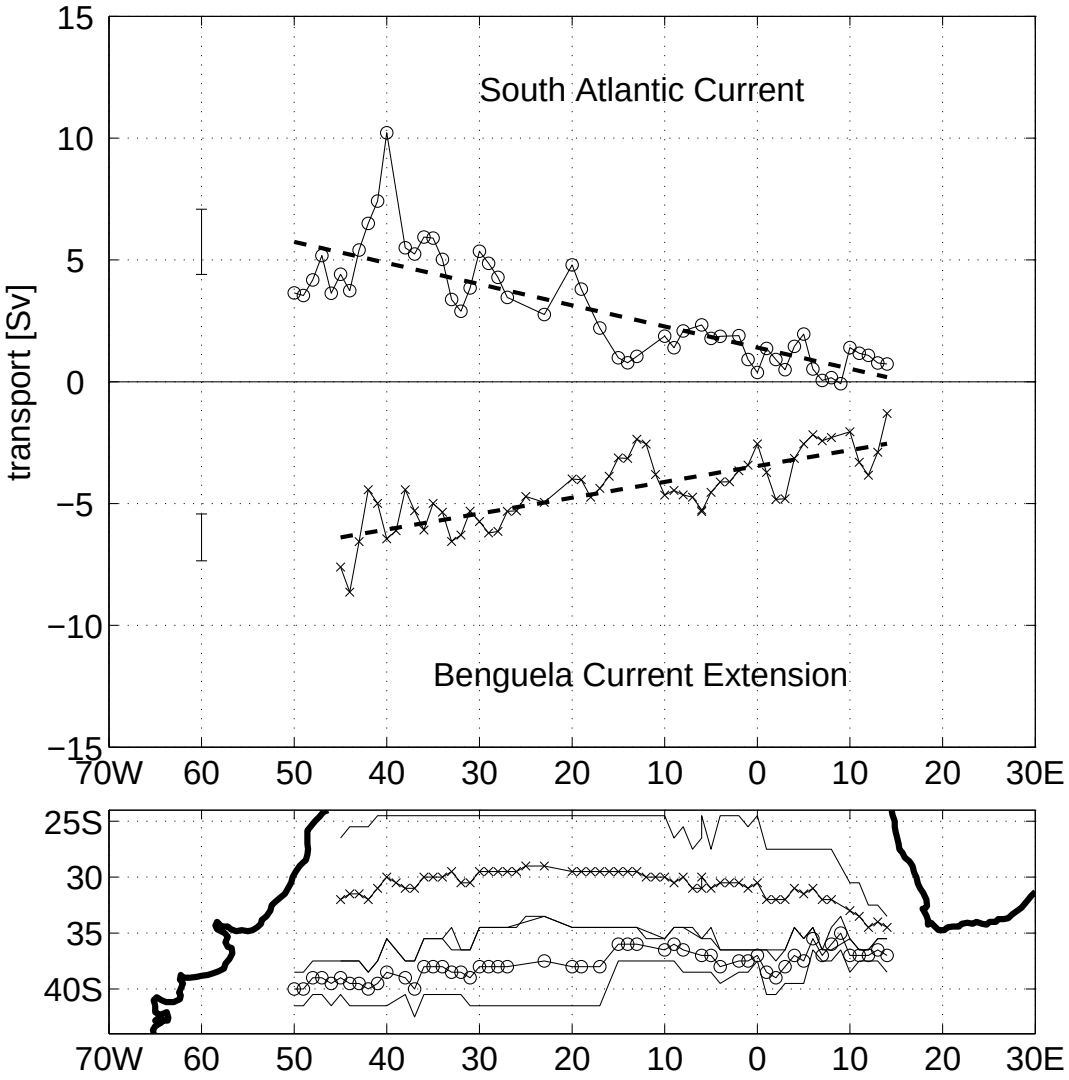

FIG. 10: Top: annual mean zonal transports of the eastward and westward currents between 800 and 1100 dbar that form the subtropical gyre in the South Atlantic. The mean was derived from objectively mapped quarterly fields of the velocity that were derived from float trajectories. The error bars to the left of the curves reflect the error of the linear fits indicated by dashed lines. The slopes and offsets of the fits are: -0.09 per degree and 1.40 for the South Atlantic Current, and 0.07 per degree and -3.46 for the Benguela Current Extension. Bottom: map depicting the center, and the meridional bounds of the two currents.

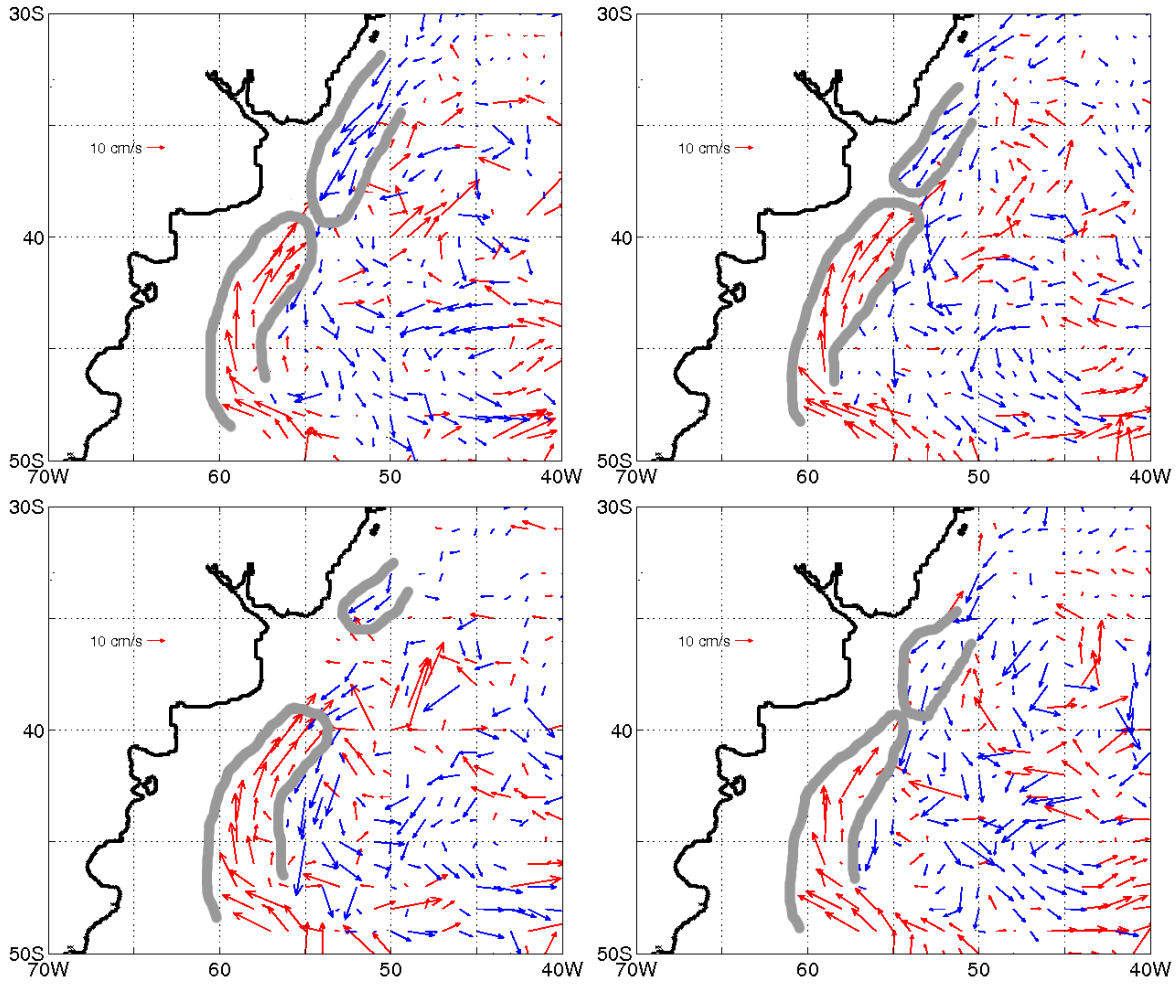

FIG. 11: Quarterly velocity vectors between 800 and 1100 dbar derived from the box-averaged velocities. Red to the north, blue to the south. The thick grey lines indicate the extents of the Brazil Current and Malvinas Current. From left to right, top to bottom: Jan-Mar, Apr-Jun, Jul-Sep, Oct-Dec.

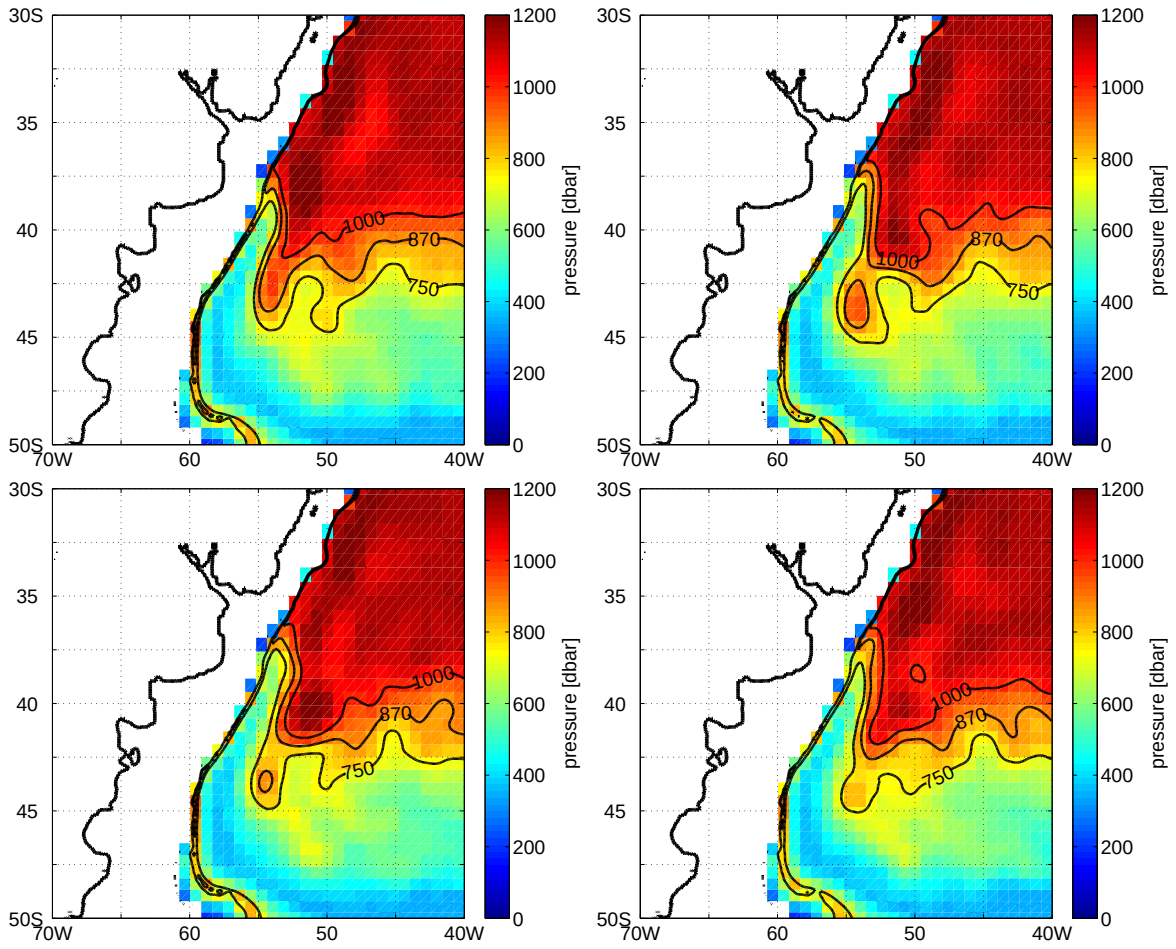

FIG. 12: Quarterly mean depth of layer 19 from HYCOM years 11-15 From left to right, top to bottom: Jan-Mar, Apr-Jun, Jul-Sep, Oct-Dec.

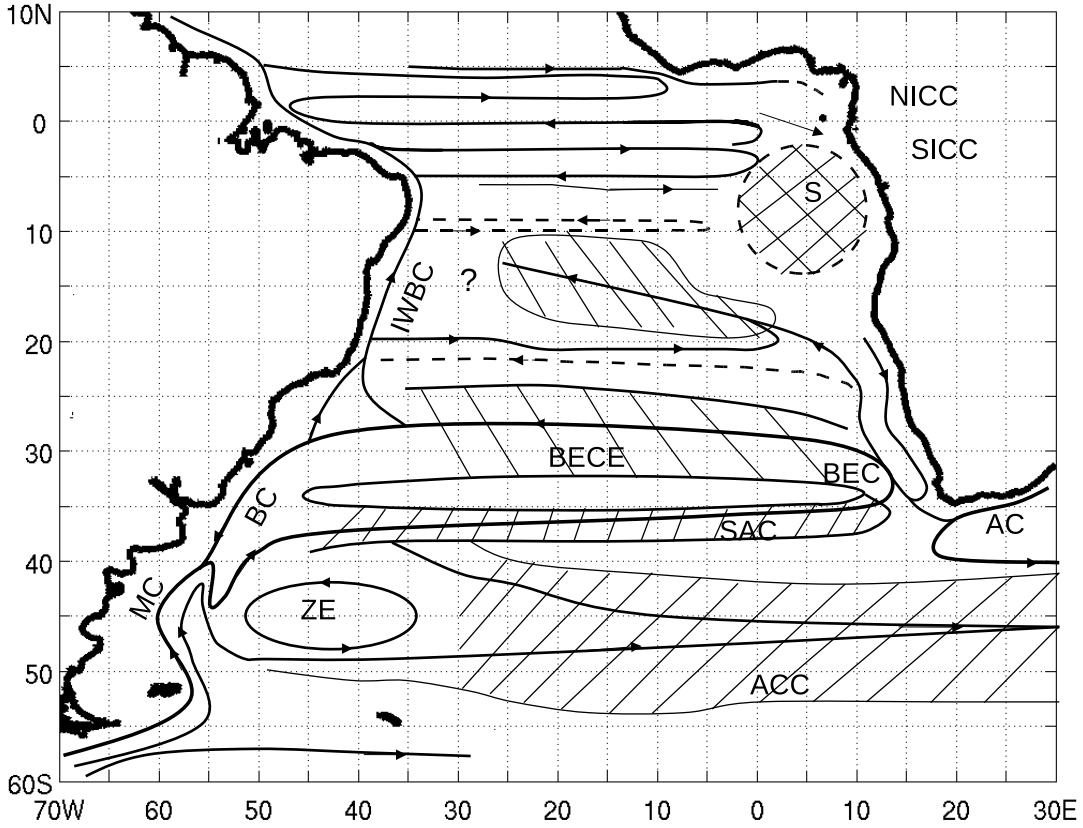

FIG. 13: Schematic of the flow field at intermediate depth based on the velocity field at 800 to 1100 dbar and the water properties at the core of the Antarctic Intermediate Water layer. Hatching from the lower left to upper right (lower right to upper left) is used for broad eastward (westward) currents The names of currents and other features are, in alphabetical order: AC = Agulhas Current, ACC = Antarctic Circumpolar Current, BC = Brazil Current, BEC = Benguela Current, BECE = Benguela Current Extension, IWBC = Intermediate Western Boundary Current, MC = Malvinas Current, NICC = Northern Intermediate Countercurrent, S = stagnant region (poorly ventilated, cross-hatched), SAC = South Atlantic Current, SICC = Southern Intermediate Countercurrent, ZE = Zappiola Eddy.